

# Transport Properties of Multiple Quantum Dots Arranged in Parallel: Results from the Bethe Ansatz

Robert M. Konik

*Department of Physics, Brookhaven National Laboratory, Upton, NY 11973*

(Dated: June 19, 2021)

In this paper we analyze transport through a double dot system connected to two external leads. Imagining each dot possessing a single active level, we model the system through a generalization of the Anderson model. We argue that this model is exactly solvable when certain constraints are placed upon the dot Coulomb charging energy, the dot-lead hybridization, and the value of the applied gate voltage. Using this exact solvability, we access the zero temperature linear response conductance both in and out of the presence of a Zeeman field. We are also able to study the finite temperature linear response conductance. We focus on universal behaviour and identify three primary features in the transport of the dots: i) a so-called RKKY Kondo effect; ii) a standard Kondo effect; and iii) interference phenomena leading to sharp variations in the conductance including conductance zeros. We are able to use the exact solvability of the dot model to characterize these phenomena quantitatively. While here we primarily consider a double dot system, the approach adopted applies equally well to N-dot systems.

PACS numbers: 72.15.Qm, 73.23.Hk, 85.35.Gv, 71.10.Pm

## I. INTRODUCTION

Quantum dot devices exhibit a wide range of strongly correlated phenomena. In the simplest of cases, single dot devices exhibit classical Kondo physics,<sup>1,2</sup> the archetype of strong correlations in impurity systems. This physics arises in dots due to their natural localization of electronic (and hence spin) degrees of freedom. Measuring transport properties provides the most effective means to probe the Kondo physics in such dots. The formation of the Abrikosov-Suhl resonance, a dynamical enhancement in the density of states at the Fermi energy, facilitates transport through the dot from one lead to the other. Manipulations of this resonance through adjustments of temperature, bias, or external fields are readily observed through monitoring the device's conductance.

At the next level of complexity are single level dots where multiple energy levels are relevant to transport. Much attention has been paid to the situation where two levels in a single dot are anomalously close.<sup>3,4,5,6</sup> In such a case the dot can be tuned through a singlet-triplet transition. On the triplet side a two stage Kondo effect can be realized.<sup>5,6</sup> Here two channels of electrons coupled with different strengths to the dot triplet successively reduce the impurity from  $S = 1$  to  $S = 1/2$  to  $S = 0$  in a two stage process.

Quantum dot devices with multiple active dots offer the same range of phenomenology as single multi-level dots but with greater versatility as level spacing and interactions are not precisely controllable within a single dot. In particular multiple quantum dot devices offer the opportunity to study non-trivial mixtures of strongly correlated physics and interference phenomena. Any Kondo physics that arises in such systems will be strongly affected by the presence of multiple tunneling paths afforded by the multiple dots. Even in the absence of interactions, multiple tunneling paths lead to richly struc-

tured transport behaviour predicated upon interference effects.

Multiple dot devices come in a number of guises. In one instance they are manufactured from gated semiconducting heterostructures.<sup>7,8,9,10</sup> An important feature that the semiconducting multi-dots share with their single dot cousins is their tunability. By adjusting voltages applied to various gates which define the dots, it is possible to change fundamental parameters of the dot system allowing experimental exploration of all of the dots' various physical regimes. In a second instance they can be constructed from carbon nanotubes.<sup>11,12</sup> With appropriate gating, carbon nanotube dots can also be made fully tunable.<sup>11,12</sup> Much of the experimental interest in multiple quantum dots comes from their possible realization as elementary qubits in a quantum computer.<sup>10,13,14</sup> As the spin degrees of freedom on the dot serve as the states of the qubit, the question of spin decoherence due to coupling with the nuclear background becomes an important question.<sup>10,13,14,15</sup> Carbon nanotube dots have the advantage that their spin decoherence times are expected to be longer due to a weaker nuclear background in carbon than in GaAs.<sup>11,12</sup>

The promised rich phenomenology and the ability to realize multiple dot devices together have led to a flurry of theoretical work in this area. Combinations of interference effects and Kondo physics in parallel dots have been studied in many works.<sup>16,17,18,19,20,21,22</sup> In response to the observations of a competition between an effective Ruderman-Kittel-Kasuya-Yosida (RKKY) coupling and a Kondo effect in a pair of double dots in series,<sup>7,8</sup> a number of works have studied the physics of RKKY effects in quantum dots.<sup>17,23,25</sup> Techniques that have been used to study multiple dots include infinite U slave boson mean field theory,<sup>16,17,18,19,24,25,26,27</sup> numerical renormalization group,<sup>16,21,24,28,29</sup> exact diagonalization,<sup>20,30</sup> appeal to asymptotic limits,<sup>4,5,23,31</sup> a perturbative renor-

malization group<sup>32</sup>, and a functional renormalization group<sup>33,34</sup>.

In this work we present a distinct approach to analyzing such systems: we study such systems under the rubric of integrability. Like the numerical renormalization group it offers exact results but with the advantage of analytic control. Integrability has long been known to be able to access *thermodynamic* properties of single level dot systems.<sup>35</sup> More recently it has been shown to be successful in computing equilibrium *transport* properties of single level quantum dots.<sup>36</sup> In particular, these techniques were able to compute the finite temperature linear response conductance over a number of decades in temperature in good agreement with the numerical renormalization group. The aim of this paper is to apply this approach to multiple quantum dots. It is an extension and elaboration of work first reported in Ref. (37).

To this end, we examine a generalized Anderson model coupling two leads ( $l = 1, 2$ ) to an array of dots in parallel:

$$\begin{aligned} \mathcal{H} = & -i \sum_{l\sigma} \int_{-\infty}^{\infty} dx c_{l\sigma}^{\dagger} \partial_x c_{l\sigma} + \sum_{\sigma\alpha} V_{l\alpha} (c_{l\sigma\alpha}^{\dagger} d_{\sigma\alpha} + \text{h.c.}) \\ & + \sum_{\sigma\alpha} \epsilon_{d\alpha} n_{\sigma\alpha} + \sum_{\alpha\alpha'} U_{\alpha\alpha'} n_{\uparrow\alpha} n_{\downarrow\alpha}. \end{aligned} \quad (1.1)$$

Here the  $c_{l\sigma}/d_{\alpha\sigma}$  specify electrons living in the leads and the dots.  $\alpha$  indexes the various levels on the dots in the system.  $V_{l\alpha}$  measures the tunneling strength between the dot level  $\alpha$  and lead  $l$ .  $U_{\alpha\alpha'}$  characterizes the Coulombic repulsion between electrons of opposite spin living in levels  $\alpha$  and  $\alpha'$ . A schematic of this Hamiltonian for two dots, i.e.  $\alpha = 1, 2$ , is given in Figure 1.

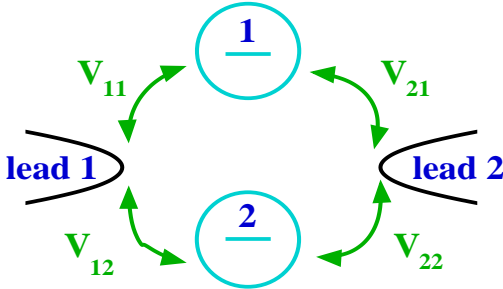


FIG. 1: A schematic of two dots in parallel.

We will argue in this paper that the above Anderson-like Hamiltonian is exactly solvable in two cases:

$$\begin{aligned} V_{1\alpha}/V_{2\alpha} &= V_{1\alpha'}/V_{2\alpha'}; \\ U_{\alpha\alpha'} &= \delta_{\alpha\alpha'} U_{\alpha}; \quad U_{\alpha}\Gamma_{\alpha} = U_{\alpha'}\Gamma_{\alpha'}; \\ U_{\alpha} + 2\epsilon_{d\alpha} &= U_{\alpha'} + 2\epsilon_{d\alpha'}; \end{aligned} \quad (1.2)$$

and

$$V_{1\alpha}/V_{2\alpha} = V_{1\alpha'}/V_{2\alpha'};$$

$$U_{\alpha\alpha'} = U; \quad \Gamma_{\alpha} = \Gamma_{\alpha'}; \quad \epsilon_{d\alpha} = \epsilon_{d\alpha'} = \epsilon_d. \quad (1.3)$$

The first condition in both cases guarantees that only a single effective channel in the leads couples to the dots. This condition is commonplace in the literature.<sup>17,18,19,20,21,29,30,32,38</sup> The second condition implies that for fixed Coulomb repulsion of the dots, the bare level separation of the two dots,  $|\epsilon_{d1} - \epsilon_{d2}|$ , is also fixed. This still permits the dot levels to be moved in unison, say by the application of a uniform gate voltage. The final condition amounts to the insistence that the energy scale associated with the charge degrees of freedom, i.e.  $\sqrt{U_i\Gamma_i}$ , must be the same on both dots. However this is not a serious constraint as we are much more interested in physics occurring on a scale associated with spin fluctuations which are not so constrained.

In the bulk of the paper, we focus this approach on studying double dots (i.e.  $\alpha = 1, 2$  in the above model). We identify a number of interesting phenomena. At the particle-hole symmetric point of the double dot system we find that the ground state of the system is a singlet *and* is characterized by a Kondo-like resonance. This implies that the RKKY interaction between the dots acts in an unusual fashion. In the standard picture, one expects either that an antiferromagnetic RKKY interaction binds the two electrons into a singlet but with any Kondo effect absent or that a ferromagnetic RKKY interaction binds the electrons into a triplet which is subsequently reduced upon Kondo screening to a doublet. But here we find neither scenario. Instead we find an effective antiferromagnetic RKKY interaction that cooperates, not competes, at an equivalent energy scale with Kondo singlet formation. We term this an RKKY Kondo effect. This RKKY effect is clearly much different than the perturbative ferromagnetic interaction<sup>39</sup> between dots appropriate for a high temperature analysis of the dot system.<sup>40</sup> Using the Bethe ansatz, we are able to describe quantitatively the associated Abrikosov-Suhl resonance together with how it evolves under applications of finite gate voltage (thus destroying particle-hole symmetry), finite magnetic field, and finite temperature.

We also identify a phenomena that we believe is underappreciated. At values of the gate voltage where the dot system is transitioning from the mixed valence regime to the empty orbital regime, the number of electrons displaced,  $n_{\text{dis}}$ , in connecting the leads to the dots is negative.  $n_{\text{dis}}$  is a sum of both the localized electrons on the dots and changes in the electron density in the leads. Our analysis allows us to argue that this second contribution to  $n_{\text{dis}}$  is finite (and negative). This phenomena is associated in general with the presence of interference and for example has also been predicted to occur in dots exhibiting Fano resonances.<sup>41</sup>

A detailed outline of the paper is as follows. It is divided in two overall parts. The first part, comprising Sections II through IV, is technical in nature. In Section II we both introduce the model of N-dots in parallel and demonstrate that it admits an exact solution via the

Bethe ansatz. To do so we construct both the one and two particle wavefunctions explicitly. This allows the extraction of the S-matrix and thus the ability to construct *implicitly* the N-particle wavefunctions through the algebraic Bethe ansatz. We also sketch briefly the *explicit* construction of the N-particle wavefunctions. This is necessary to ensure the posited Bethe ansatz wavefunctions are indeed eigenfunctions of the dot Hamiltonian. Finally in Section II we provide a general analysis of the Bethe ansatz equations in the continuum limit both at zero and finite temperature.

In Section III we sketch how the transport properties of the double dot can be accessed via the Bethe ansatz equations. We do so on the same basis that the magnetoconductance was computed in the Kondo model.<sup>42</sup> There the scattering phase of an electron off the spin impurity was computed by analyzing the  $1/L$  (where  $L$  is the system size) corrections of the Bethe ansatz equations. Here the analysis is more involved as Anderson-type models have non-trivial excitations involving both charge and spin degrees of freedom (unlike the Kondo model where the charge sector decouples). We, however, are still able to relate the scattering phase to an impurity density of states. As this latter quantity is readily extracted from the Bethe ansatz equations, we are in position to characterize the transport through the dot. In Section III we sketch how this proceeds both at zero and finite temperature.

Up to this point in the article, we have made no attempt to provide specific solutions to the integral equations arising out of the analysis of the Bethe ansatz quantization condition. In Section IV of the paper this changes. We both specialize to the case of two dots and we outline how the equations describing transport through two-dot systems can be solved analytically in the two particular limits of large and small bare level separation, i.e.  $|\epsilon_{d1} - \epsilon_{d2}| \gg V_{1,2}^2$  and  $|\epsilon_{d1} - \epsilon_{d2}| \ll V_{1,2}^2$ . This ends the technical portion of the paper.

In the second part of the paper, Sections V through VII, we discuss the various features of transport arising in a double parallel dot system. These sections can be read (mostly) independently from the Bethe ansatz analysis in the paper's first part. In Section V we study zero temperature transport both in and out of an applied Zeeman field. In zero field we study the conductance through the double dots as a function of gate voltage. We identify three regions of gate voltage: i) near the particle-hole symmetric point where two electrons sit on the dots and where what we term an RKKY Kondo effect is present; ii) a region in gate voltage where one electron sits on the dots and a standard Kondo effect takes place; and iii) a region in gate voltage marking the transition between a mixed valence and empty orbital regime where marked interference effects are present. We then study how these various phenomena are affected by the introduction of a Zeeman field. In Section VI we study the finite temperature linear response conductance at the particle-hole symmetric point (i.e. how the introduction of a tempera-

ture destroys the RKKY Kondo effect). In Section VII we end the paper considering two items. We first examine how the Friedel sum rule operates in the region where strong interference effects are present. And second we consider how breaking the integrability constraints, i.e. Eqns. (1.2) and (1.3), affects the physics we have discussed in the manuscript. On this last point we conclude that the effects are in general perturbative, i.e. small violations of the constraints leads only to small changes in the physics.

## II. EXACT SOLVABILITY OF N-DOTS IN PARALLEL

### A. Integrability of Model: Bethe Ansatz Equations

To begin to analyze the model in Eqn. (1.1) we first map the problem to an Anderson model involving a single effective lead. To do so we need to assume the ratio of left/right lead couplings are equal, i.e.  $V_{1\alpha}/V_{2\alpha} = V_{1\alpha'}/V_{2\alpha'}$ . Writing  $c_{e/o} = (V_{1/2\alpha}c_1 \pm V_{2/1\alpha}c_2)/\sqrt{2\Gamma_\alpha}$ , with  $\Gamma_\alpha = (V_{1\alpha}^2 + V_{2\alpha}^2)/2$ , the Hamiltonian factorizes into an even and an odd sector:

$$\begin{aligned}\mathcal{H}_e &= -i \sum_{l\sigma} \int_{-\infty}^{\infty} dx \, c_{e\sigma}^\dagger \partial_x c_{e\sigma} + \sum_{\sigma\alpha} \sqrt{2\Gamma_\alpha} (c_{e\sigma\alpha}^\dagger d_{\sigma\alpha} + \text{h.c.}) \\ &\quad + \sum_{\sigma\alpha} \epsilon_{d\alpha} n_{\sigma\alpha} + \sum_{\alpha\alpha'} U_{\alpha\alpha'} n_{\uparrow\alpha} n_{\downarrow\alpha}; \\ \mathcal{H}_o &= -i \sum_{l\sigma} \int_{-\infty}^{\infty} dx \, c_{o\sigma}^\dagger \partial_x c_{o\sigma}.\end{aligned}\quad (2.1)$$

Only the even Hamiltonian, coupling directly to the dot degrees of freedom, is non-trivial.

To determine under what conditions  $\mathcal{H}_e$  is exactly solvable by Bethe ansatz we compute both the one and two electron eigenstates. The one particle wave function takes the form,

$$|\psi_\sigma\rangle = \left[ \int_{-\infty}^{\infty} dx \{g_\sigma(x) c_\sigma^\dagger(x)\} + e_{\alpha\sigma} d_{\alpha\sigma}^\dagger \right] |0\rangle. \quad (2.2)$$

We solve the Schrödinger equation,  $\mathcal{H}_e|\psi\rangle = q|\psi\rangle$ , and find  $g(q)$  is of the form,

$$g_\sigma(x) = \theta(x) e^{iqx + i\frac{\delta(q)}{2}} + \theta(-x) e^{iqx - i\frac{\delta(q)}{2}}, \quad (2.3)$$

with  $\delta(q)$  the scattering phase of the electron off the dot array equaling,

$$\delta(q) = -2 \tan^{-1} \left( \sum_{\alpha} \frac{\Gamma_\alpha}{q - \epsilon_{d\alpha}} \right). \quad (2.4)$$

The total scattering phase is a sum of the *arguments* of  $\tan^{-1}$  of scattering phases off the individual dots in the system.

The two particle eigenfunction in the  $S_z = 0$  sector takes the form

$$|\psi\rangle = \left[ \int_{-\infty}^{\infty} dx_1 dx_2 g(x_1, x_2) c_\uparrow^\dagger(x_1) c_\downarrow^\dagger(x_2) + \sum_{\alpha} \int_{-\infty}^{\infty} dx \right.$$

$$[e_\alpha(x)(c_\uparrow^\dagger(x)d_{\alpha\downarrow}^\dagger - c_\downarrow^\dagger(x)d_{\uparrow\alpha}^\dagger)] + \sum_{\alpha\alpha'} f_{\alpha\alpha'} d_{\uparrow\alpha}^\dagger d_{\downarrow\alpha'}^\dagger] |0\rangle. \quad (2.5)$$

Again solving the Schrödinger equation  $\mathcal{H}_e|\psi\rangle = (q + p)|\psi\rangle$  gives  $g(x_1, x_2)$  to be

$$g(x_1, x_2) = g_q(x_1)g_p(x_2)\phi(x_1 - x_2) + g_p(x_1)g_q(x_2)\phi(x_2 - x_1). \quad (2.6)$$

Here  $g_{q/p}(x)$  and  $e_{q/p}$  are the coefficients appearing in the one particle wavefunction corresponding to energies  $q/p$ .  $\phi(x)$  governs the scattering when two electrons are interchanged. It takes the form  $\phi(x) = 1 + i\gamma(q, p)\text{sign}(x)$ . We find that  $\gamma(q, p)$  must satisfy for arbitrary  $\alpha$ ,

$$\gamma(q, p) = \frac{1}{2} \frac{1}{q - p} \sum_{\alpha'} \frac{p_\alpha q_{\alpha'} + p_{\alpha'} q_\alpha}{p_{\alpha'} q_{\alpha'}} \times \frac{2\Gamma_{\alpha'} U_{\alpha\alpha'}}{\epsilon_{d\alpha} + \epsilon_{d\alpha'} + U_{\alpha\alpha'} - q - p}, \quad (2.7)$$

where  $p_\alpha/q_\alpha = p - \epsilon_{d\alpha}/q - \epsilon_{d\alpha}$ . For consistency,  $\gamma(p, q)$  must be independent of a particular value of  $\alpha$ . This only happens if one of two sets of conditions holds:

case i:

$$U_{\alpha\alpha'} = \delta_{\alpha\alpha'} U_\alpha; \quad U_\alpha \Gamma_\alpha = U_{\alpha'} \Gamma_{\alpha'}; \quad (2.8)$$

$$U_\alpha + 2\epsilon_{d\alpha} = U_{\alpha'} + 2\epsilon_{d\alpha'};$$

case ii:

$$U_{\alpha\alpha'} = U; \quad \Gamma_\alpha = \Gamma_{\alpha'}; \quad \epsilon_{d\alpha} = \epsilon_{d\alpha'} = \epsilon_d. \quad (2.9)$$

Case i) would be appropriate to describing well separated single level dots while case ii) would be appropriate to describing a single dot with degenerate levels.

Exact solvability is predicated on how  $\gamma(q, p)$  determines the scattering matrix of the two electrons. The scattering matrix has the general spin (SU(2)) invariant form

$$S_{\sigma_1\sigma_2}^{\sigma'_1\sigma'_2} = b(p, q) I_{\sigma_1\sigma_2}^{\sigma'_1\sigma'_2} + c(p, q) P_{\sigma_1\sigma_2}^{\sigma'_1\sigma'_2}, \quad (2.10)$$

where here  $\{\sigma_1, \sigma_2\}/\{\sigma'_1, \sigma'_2\}$  represent the incoming and outgoing spins. Here  $I_{\sigma_1\sigma_2}^{\sigma'_1\sigma'_2} = \delta_{\sigma_1\sigma'_1} \delta_{\sigma_2\sigma'_2}$  is the identity matrix while  $P_{\sigma_1\sigma_2}^{\sigma'_1\sigma'_2} = \delta_{\sigma_1\sigma'_2} \delta_{\sigma_2\sigma'_1}$  is the permutation matrix. The coefficients,  $b(p, q)$  and  $c(p, q)$ , are determined by  $\gamma(p, q)$  from the two relations

$$b(p, q) - c(p, q) = \frac{\phi(x_1 - x_2)}{\phi(x_2 - x_1)} = \frac{1 + i\gamma(p, q)}{1 - i\gamma(p, q)}$$

$$b(p, q) + c(p, q) = 1. \quad (2.11)$$

The first relation results from the two particle eigenfunction in the  $S_z = 0$  sector solved above while the second

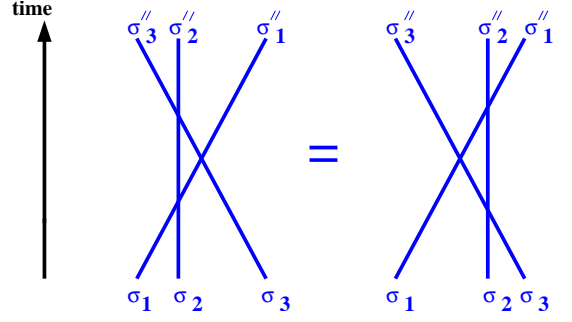


FIG. 2: A graphical representation of the Yang-Baxter equation. Three particles  $\sigma_1, \sigma_2$ , and  $\sigma_3$  scatter into  $\sigma'_1, \sigma'_2$ , and  $\sigma'_3$  in two different ways. Under the Yang-Baxter relation, the two scattering processes are equivalent.

relation arises from the corresponding eigenfunction in the  $S_z = \pm 1$  sector where interactions between spins are trivial.

In order for the Hamiltonian  $\mathcal{H}_e$  to be integrable, the above S-matrix must satisfy the Yang-Baxter relation. The Yang-Baxter relation governs the scattering of three electrons,  $\sigma_1, \sigma_2$ , and  $\sigma_3$ . It enforces the equivalency of different scattering orders.  $\sigma_1$  may first scatter off  $\sigma_2$  and then  $\sigma_3$  followed by a scattering of  $\sigma_2$  and  $\sigma_3$  or  $\sigma_2$  and  $\sigma_3$  may scatter first followed by successive scattering of  $\sigma_1$  off  $\sigma_2$  and  $\sigma_3$ . This is graphically encoded in Figure 2. Algebraically it is given by

$$S_{\sigma_1\sigma_2}^{\sigma'_1\sigma'_2}(p_1, p_2) S_{\sigma'_1\sigma'_3}^{\sigma''_1\sigma''_3}(p_1, p_3) S_{\sigma'_2\sigma'_3}^{\sigma''_2\sigma''_3}(p_2, p_3) = S_{\sigma_2\sigma_3}^{\sigma'_2\sigma'_3}(p_2, p_3) S_{\sigma_1\sigma'_3}^{\sigma'_1\sigma''_3}(p_1, p_3) S_{\sigma'_1\sigma'_2}^{\sigma''_1\sigma''_2}(p_1, p_2). \quad (2.12)$$

If this relation holds, the scattering among three particles is independent of the order in which the particles scatter among one another. For an SU(2) invariant system, the Yang-Baxter relationship reduces to the simple condition,<sup>35</sup>

$$b(p, q)/c(p, q) = g(p) - g(q), \quad (2.13)$$

where  $g(p)$  is some function. In case i),  $g(p)$  is given by

$$g(p) = \frac{(p - \epsilon_{d\alpha} - U_{\alpha\alpha}/2)^2}{2\Gamma_\alpha U_{\alpha\alpha}}; \quad (2.14)$$

while in case ii),  $g(p)$  equals

$$g(p) = \frac{(p - \epsilon_d - U/2)^2}{2U \sum_\alpha \Gamma_\alpha}. \quad (2.15)$$

In the second case,  $g(p)$  is equivalent to a single dot with level broadening  $\Gamma = \sum_\alpha \Gamma_\alpha$ .

Having determine under what conditions the dot-lead Hamiltonian is exactly solvable, we are now in a position to construct  $N$ -particle eigenstates in a controlled fashion. An eigenfunction with spin  $2S_z = N - 2M$ , is characterized by a sea of  $N$  electrons each carrying momenta

$\{q_i\}_{i=1}^N$  and so total energy  $E = \sum_i q_i$ . In a periodic system of length  $L$ , integrability allows us to write down in a compact form the  $k_i$ -quantization conditions (the Bethe ansatz equations):

$$e^{iq_j L + i\delta(q_j)} = \prod_{\alpha=1}^M \frac{g(q_j) - \lambda_\alpha + i/2}{g(q_j) - \lambda_\alpha - i/2};$$

$$\prod_{j=1}^N \frac{\lambda_\alpha - g(q_j) + i/2}{\lambda_\alpha - g(q_j) - i/2} = - \prod_{\beta=1}^M \frac{\lambda_\alpha - \lambda_\beta + i}{\lambda_\alpha - \lambda_\beta - i}. \quad (2.16)$$

These equations are identical to those for the ordinary Anderson model<sup>35</sup> but for the form of  $\delta(q)$  (here given in Eqn. (2.4)). The  $M$ - $\lambda_\alpha$  appearing in the above equations are indicative of the spin degrees of freedom.

The Bethe ansatz equations are derived in the same

fashion (using the algebraic Bethe ansatz) as described in Ref. (35). However it is important to also explicitly construct the  $N$ -particle wavefunctions. There is an *a priori* possibility that even though the integrability conditions (i.e. Eqn. (2.13)) are satisfied, the  $N$ -particle wavefunctions posited by the Bethe ansatz are not actual eigenfunctions of the Hamiltonian. This possibility has been seen previously in Hubbard models with more than two species of electrons.<sup>43</sup> In such a case what spoils integrability is the possibility that more than two electrons sit on the same site. A similar possibility thus exists here where more than two electrons can sit on the dots.

For simplicity, we only consider the case where two dots are involved. The  $N$ -particle wavefunctions with  $M$   $\downarrow$  electrons (assuming  $N > M > 2$ ) in this case take the form

$$\begin{aligned} |\psi_{N,M}\rangle = & \int dx_1 \cdots dx_N g(x_1, \dots, x_N) c_{\downarrow}^{\dagger}(x_1) \cdots c_{\downarrow}^{\dagger}(x_M) c_{\uparrow}^{\dagger}(x_{M+1}) \cdots c_{\uparrow}^{\dagger}(x_N) \\ & + \sum_{\alpha=1,2, \sigma=\uparrow, \downarrow} \int dx_1 \cdots dx_{M-s_{\downarrow}(\sigma)} dx_{M+1} \cdots dx_{N-s_{\downarrow}(\sigma)} e_{\sigma\alpha}(x_1, \dots, x_{M-s_{\downarrow}(\sigma)}, x_{M+1}, \dots, x_{N-s_{\downarrow}(\sigma)}) \\ & \quad \times c_{\downarrow}^{\dagger}(x_1) \cdots c_{\downarrow}^{\dagger}(x_{M-s_{\downarrow}(\sigma)}) c_{\uparrow}^{\dagger}(x_{M+1}) \cdots c_{\uparrow}^{\dagger}(x_{N-s_{\downarrow}(\sigma)}) d_{\sigma\alpha}^{\dagger} \\ & + \sum_{\sigma\sigma'\alpha\alpha'} \int dx_1 \cdots dx_{M-s_{\downarrow}(\sigma)-s_{\downarrow}(\sigma')} dx_{M+1} \cdots dx_{N-s_{\downarrow}(\sigma)-s_{\downarrow}(\sigma')} \\ & \quad \times f_{\sigma\sigma'\alpha\alpha'}(x_1, \dots, x_{M-s_{\downarrow}(\sigma)-s_{\downarrow}(\sigma')}, x_{M+1}, \dots, x_{N-s_{\downarrow}(\sigma)-s_{\downarrow}(\sigma')}) \\ & \quad \times c_{\downarrow}^{\dagger}(x_1) \cdots c_{\downarrow}^{\dagger}(x_{M-s_{\downarrow}(\sigma)-s_{\downarrow}(\sigma')}) c_{\uparrow}^{\dagger}(x_{M+1}) \cdots c_{\uparrow}^{\dagger}(x_{N-s_{\downarrow}(\sigma)-s_{\downarrow}(\sigma')}) d_{\sigma\alpha}^{\dagger} d_{\sigma'\alpha'}^{\dagger} \\ & + \sum_{\sigma\sigma'\sigma''\alpha\alpha'\alpha''} \int dx_1 \cdots dx_{M-s_{\downarrow}(\sigma)-s_{\downarrow}(\sigma')-s_{\downarrow}(\sigma'')} dx_{M+1} \cdots dx_{N-s_{\downarrow}(\sigma)-s_{\downarrow}(\sigma')-s_{\downarrow}(\sigma'')} \\ & \quad \times r_{\sigma\sigma'\sigma''\alpha\alpha'\alpha''}(x_1, \dots, x_{M-s_{\downarrow}(\sigma)-s_{\downarrow}(\sigma')-s_{\downarrow}(\sigma'')}, x_{M+1}, \dots, x_{N-s_{\downarrow}(\sigma)-s_{\downarrow}(\sigma')-s_{\downarrow}(\sigma'')}) \\ & \quad \times c_{\downarrow}^{\dagger}(x_1) \cdots c_{\downarrow}^{\dagger}(x_{M-s_{\downarrow}(\sigma)-s_{\downarrow}(\sigma')-s_{\downarrow}(\sigma'')}) c_{\uparrow}^{\dagger}(x_{M+1}) \cdots c_{\uparrow}^{\dagger}(x_{N-s_{\downarrow}(\sigma)-s_{\downarrow}(\sigma')-s_{\downarrow}(\sigma'')}) d_{\sigma\alpha}^{\dagger} d_{\sigma'\alpha'}^{\dagger} d_{\sigma''\alpha''}^{\dagger} \\ & + \int dx_1 \cdots dx_{M-2} dx_{M+1} \cdots dx_{N-2} h(x_1, \dots, x_{M-2}, x_{M+1}, \dots, x_{N-2}) \\ & \quad \times c_{\downarrow}^{\dagger}(x_1) \cdots c_{\downarrow}^{\dagger}(x_{M-2}) c_{\uparrow}^{\dagger}(x_{M+1}) \cdots c_{\uparrow}^{\dagger}(x_{N-2}) d_{\uparrow 1}^{\dagger} d_{\downarrow 1}^{\dagger} d_{\uparrow 2}^{\dagger} d_{\downarrow 2}^{\dagger}, \quad (2.17) \end{aligned}$$

where  $s_{\downarrow}(\downarrow) = s_{\uparrow}(\uparrow) = 1$  and  $s_{\downarrow}(\uparrow) = s_{\uparrow}(\downarrow) = 0$ . The different terms of the wavefunction correspond to different numbers of electrons sitting on the dots. We look for eigenstates with total energy  $E = \sum_{i=1}^N q_i$  where the  $q_i$

are single particle energies. Under the Bethe ansatz the coefficients,  $g(x_i)$ ,  $e_{\sigma\alpha}(x_i)$ ,  $f_{\sigma\sigma'\alpha\alpha'}(x_i)$ ,  $r_{\sigma\sigma'\sigma''\alpha\alpha'\alpha''}(x_i)$ , and  $h(x_i)$  take the form

$$g(x_1, \dots, x_N) = \sum_{\sigma \in S_N} \prod g_{q_{\sigma(i)}}(x_i) \cdot A_{N,M}(x_i|\sigma);$$

$$e_{\sigma\alpha}(x_1, \dots, x_{M-s_{\downarrow}(\sigma)}, x_{M+1}, \dots, x_{N-s_{\downarrow}(\sigma)}) = \sum_{\sigma \in S_N} \prod_{i=1}^{M-s_{\downarrow}(\sigma)} g_{q_{\sigma(i)}}(x_i) \prod_{i=M+1}^{N-s_{\downarrow}(\sigma)} g_{q_{\sigma(i)}}(x_i)$$

$$\begin{aligned}
& \times \prod_{i=M-s_{\downarrow}(\sigma)+1}^M e_{q_{\sigma(i)}} \prod_{i=N-s_{\uparrow}(\sigma)+1}^N e_{q_{\sigma(i)}} B_{\sigma\alpha N,M}(x_1, \dots, x_{M-s_{\downarrow}(\sigma)}, x_{M+1}, \dots, x_{N-s_{\uparrow}(\sigma)} | \sigma); \\
& f_{\sigma\sigma'\alpha\alpha'}(x_1, \dots, x_{M-s_{\downarrow}(\sigma)-s_{\downarrow}(\sigma')}, x_{M+1}, \dots, x_{N-s_{\uparrow}(\sigma)-s_{\uparrow}(\sigma')}) = \\
& \times \sum_{\sigma \in S_N} \prod_{i=1}^{M-s_{\downarrow}(\sigma)-s_{\downarrow}(\sigma')} g_{q_{\sigma(i)}}(x_i) \prod_{i=M+1}^{N-s_{\uparrow}(\sigma)-s_{\uparrow}(\sigma')} g_{q_{\sigma(i)}}(x_i) \\
& \times \prod_{i=M-s_{\downarrow}(\sigma)-s_{\downarrow}(\sigma')+1}^M e_{q_{\sigma(i)}} \prod_{i=N-s_{\uparrow}(\sigma)-s_{\uparrow}(\sigma')+1}^N e_{q_{\sigma(i)}} \\
& \times C_{\sigma\sigma'\alpha\alpha' N,M}(x_1, \dots, x_{M-s_{\downarrow}(\sigma)-s_{\downarrow}(\sigma')}, x_{M+1}, \dots, x_{N-s_{\uparrow}(\sigma)-s_{\uparrow}(\sigma')} | \sigma); \\
& r_{\sigma\sigma'\sigma''\alpha\alpha'\alpha''}(x_1, \dots, x_{M-s_{\downarrow}(\sigma)-s_{\downarrow}(\sigma')-s_{\downarrow}(\sigma'')}, x_{M+1}, \dots, x_{N-s_{\uparrow}(\sigma)-s_{\uparrow}(\sigma')-s_{\uparrow}(\sigma'')}) = \\
& \times \sum_{\sigma \in S_N} e_{q_{\sigma(i)}} \prod_{i=1}^{M-s_{\downarrow}(\sigma)-s_{\downarrow}(\sigma')-s_{\downarrow}(\sigma'')} g_{q_{\sigma(i)}}(x_i) \prod_{i=M+1}^{N-s_{\uparrow}(\sigma)-s_{\uparrow}(\sigma')-s_{\uparrow}(\sigma'')} g_{q_{\sigma(i)}}(x_i) \\
& \times \prod_{i=M-s_{\downarrow}(\sigma)-s_{\downarrow}(\sigma')-s_{\downarrow}(\sigma'')+1}^M e_{q_{\sigma(i)}} \prod_{i=N-s_{\uparrow}(\sigma)-s_{\uparrow}(\sigma')-s_{\uparrow}(\sigma'')+1}^N e_{q_{\sigma(i)}} \\
& \times D_{\sigma\sigma'\sigma''\alpha\alpha'\alpha'' N,M}(x_1, \dots, x_{M-s_{\downarrow}(\sigma)-s_{\downarrow}(\sigma')-s_{\downarrow}(\sigma'')}, x_{M+1}, \dots, x_{N-s_{\uparrow}(\sigma)-s_{\uparrow}(\sigma')-s_{\uparrow}(\sigma'')}) | \sigma); \\
& h(x_1, \dots, x_{M-2}, x_{M+1}, \dots, x_{N-2}) = \sum_{\sigma \in S_N} e_{q_{\sigma(i)}} \prod_{i=1}^{M-2} g_{q_{\sigma(i)}}(x_i) \prod_{i=M+1}^{N-2} g_{q_{\sigma(i)}}(x_i) \\
& \times E_{N,M}(x_1, \dots, x_{M-2}, x_{M+1}, \dots, x_{N-2} | \sigma). \tag{2.18}
\end{aligned}$$

Here  $\sum_{\sigma \in S_N}$  is a sum over the permutations of  $N$ .  $g_q(x)$  is the electron portion of the single particle eigenstate defined in (2.3) with energy  $q$ . Similarly  $e_q$  is the dot portion of this same wavefunction. The coefficients  $A_{N,M}$  through  $E_{N,M}$  depend upon both  $\sigma$  and the relative ordering of the  $x_i$  (for example,  $A_{N,M}$  only changes value as the  $x_i$  cross one another). Their forms are analogous to those of the Hubbard model detailed in Ref. (44).

By direct substitution we check that this posited form of the wavefunction does indeed correspond to an eigenfunction of the Hamiltonian. While straightforward, the associated algebra is tedious and so is suppressed.

While we have only consider two dots in parallel, we can easily generalize to  $N$ -dots. In order for  $N$ -dots to be integrable we again require that  $V_{1\alpha}/V_{2\alpha} = V_{1\alpha'}/V_{2\alpha'}$  for all  $\alpha$  and  $\alpha'$  and that constraints analogous to those in Eqns. (2.7) and (2.8) are satisfied. This type of generalization is akin to the multi-lead generalizations of the single level Anderson model found in Refs. 45 and 46.

## B. Analysis of Bethe Ansatz Equations

### 1. Description at $T = 0$

$N$ -particle states with spin projection,  $2S_z = N - 2M$ , of the dot-lead system in general consists of a multitude of different types of solutions for the  $q$ 's appearing in the Bethe ansatz quantization conditions of Eqn. (2.15). But at  $T = 0$  only two solutions are relevant for the ground state. The ground state at  $T = 0$  is composed of 1)  $N-2M$  real values of  $q$  and 2)  $2M$  complex values of  $q$  interlinked to  $M$  real values of  $\lambda$  according to the rule

$$q_{\pm}(\lambda) = x(\lambda) \pm iy(\lambda); \quad g(q_{\pm}(\lambda)) = \lambda \pm i/2. \tag{2.19}$$

In the continuum limit, densities  $\rho(q)$  and  $\sigma(\lambda)$  describing the distributions of  $q$  and  $\lambda$  respectively may be derived<sup>35</sup>

$$\begin{aligned}
\rho(q) &= \frac{1}{2\pi} + \frac{\Delta(q)}{L} + g'(q) \int_{\tilde{Q}}^{\tilde{Q}} d\lambda a_1(g(q) - \lambda) \sigma(\lambda); \\
\sigma(\lambda) &= -\frac{x'(\lambda)}{\pi} + \frac{\tilde{\Delta}(\lambda)}{L} - \int_{\tilde{Q}}^{\tilde{Q}} d\lambda' a_2(\lambda' - \lambda) \sigma(\lambda') \\
&\quad - \int_{-D}^B dq a_1(\lambda - g(q)) \rho(q), \tag{2.20}
\end{aligned}$$

where

$$\begin{aligned}\Delta(q) &= \frac{1}{2\pi} \partial_q \delta(q); \\ \tilde{\Delta}(\lambda) &= -\frac{1}{\pi} \partial_\lambda \text{Re} \delta(x(\lambda) + iy(\lambda)); \\ a_n(x) &= \frac{1}{2\pi} \partial_x \theta_n(x) = \frac{2n}{\pi} \frac{1}{(n^2 + 4x^2)}.\end{aligned}\quad (2.21)$$

In the equations for the charge,  $\rho(q)$ , and spin,  $\sigma(\lambda)$ , distributions appear the Fermi surfaces,  $Q$  and  $B$ , and “band” bottoms  $\tilde{Q}$  and  $-D$ . These mark out the range of  $q$  and  $\lambda$  over which excitations appear in the ground state.  $-D$  is the lower band edge of the charge excitations. As each  $\lambda$  has two associated complex  $q$ ’s, we expect  $q_{q+}(\tilde{Q}) + q_{q-}(\tilde{Q}) = 2x(\tilde{Q}) = -2D$ , thus determining  $\tilde{Q}$ .<sup>35</sup> The Fermi surfaces  $Q$  and  $B$  are fixed by insisting that the overall spin and particle number,

$$\begin{aligned}N - 2M &= L \int_{-D}^B dq \rho(q); \\ M &= L \int_Q^{\tilde{Q}} d\lambda \sigma(\lambda),\end{aligned}\quad (2.22)$$

are reproduced.

In understanding transport properties we will want to construct electronic-like excitations (even if zero-energy) about this ground state. These excitations are in turn related to specific solutions,  $q$  and  $\lambda$ , of the Bethe ansatz equations. If for example we add an electron to the system, i.e. take  $N \rightarrow N + 1$ , to effect this change, we must add a real  $q$ -state as well as a  $\lambda$ -hole. Thus we must parameterize the energies,  $\epsilon_q(q)$  and  $\epsilon_\lambda(\lambda)$  of these excitations. Equations governing these energies are easily derivable (see Ref. (36)) and are given by

$$\begin{aligned}\epsilon_q(q) &= q - \frac{H}{2} - \int_Q^{\tilde{Q}} d\lambda \epsilon_\lambda(\lambda) a_1(\lambda - g(q)); \\ \epsilon_\lambda(\lambda) &= 2x(\lambda) - \int_Q^{\tilde{Q}} d\lambda' \epsilon_\lambda(\lambda') a_2(\lambda' - \lambda) \\ &\quad + \int_{-D}^B g'(q) \epsilon_q(q) a_1(g(q) - \lambda).\end{aligned}\quad (2.23)$$

$\epsilon_q(q)$  is a monotonically increasing function that is equal to zero at the  $q$ -Fermi surface, i.e.  $\epsilon_q(B) = 0$ . For  $q > B$ ,  $\epsilon_q(q) > 0$  indicating it costs energy,  $\epsilon_q(q)$ , to add a state above the  $q$ -Fermi surface while for  $q < B$ ,  $\epsilon_q(q) < 0$ , indicating it costs energy to add a hole below the Fermi surface. Similar consideration hold for  $\epsilon_\lambda$  (although here  $\epsilon_\lambda$  is a monotonically decreasing function which passes through 0 at  $\lambda = Q$ ).

## 2. Description at Finite $T$

The description of the system at finite temperature is considerably more involved. At finite  $T$ , an infinite

hierarchy of excitations of the Bethe ansatz equations must be considered. The two coupled integral equations at  $T = 0$  are replaced by an a correspondingly infinite set. These equations are closely related to those analyzed in Ref. (35,36). However some important differences are present and so we give the description of the system at finite temperature in some detail.

At finite temperature, the possible excitations of the system fall into three classes

**i) real  $q$ :** As we have already seen, such solutions to the Bethe ansatz equations appear in the zero temperature ground state at finite  $H$ .

**ii) n-spin complex with  $2n$  associated complex  $q$ ’s:** The n-spin complex groups together  $n$  different  $\lambda$ ’s according to the rule

$$\lambda^{nj} = \lambda^n + i\left(\frac{n+1}{2} - j\right), \quad j = 1, \dots, n.$$

Here  $\lambda^n$ , the centre of the complex, is a real number. For each  $\lambda^{nj}$ , there are two associated  $q$ ’s:

$$\begin{aligned}g(q^{+nj}) &= \lambda^n + i\left(\frac{n}{2} + 1 - j\right); \\ g(q^{-nj}) &= \lambda^n + i\left(\frac{n}{2} - j\right).\end{aligned}$$

The simplest of this type of complex ( $n = 1$ ), as we have already seen, fills the  $H = T = 0$  ground state.

**iii) n-spin complex with no associated  $q$ ’s:** As in case ii), the spin complex groups together  $n$  different  $\lambda$ ’s according to

$$\lambda^{nj} = \lambda^n + i\left(\frac{n+1}{2} - j\right), \quad j = 1, \dots, n.$$

However here there are no associated  $q$ ’s.

These excitations are governed by the following set of density equations describing their occupancies at finite  $T$  (akin to Eqn. (2.16) for the simpler  $T = 0$  case)

$$\begin{aligned}\rho_p(q) + \rho_h(q) &= \frac{1}{2\pi} + \frac{\Delta(q)}{L} \\ &+ g'(q) \sum_{n=1}^{\infty} \int_{-\infty}^{\infty} d\lambda a_n(g(q) - \lambda) (\sigma_{pn}(\lambda) + \sigma'_{pn}(\lambda)); \\ \sigma_{hn}(\lambda) &= -\frac{x'_n(\lambda)}{\pi} + \frac{\tilde{\Delta}_n(\lambda)}{L} \\ &- \int_{-\infty}^{\infty} a_n(\lambda - g(q)) \rho_p(q) \\ &- \sum_{m=1}^{\infty} \int_{-\infty}^{\infty} d\lambda' A_{nm}(\lambda - \lambda') \sigma_{pm}(\lambda'); \\ \sigma'_{hn}(\lambda) &= \int_{-\infty}^{\infty} a_n(\lambda - g(q)) \rho_p(q) \\ &- \sum_{m=1}^{\infty} \int_{-\infty}^{\infty} d\lambda' A_{nm}(\lambda - \lambda') \sigma'_{pm}(\lambda');\end{aligned}\quad (2.24)$$

where  $x_n(\lambda)$  and  $\tilde{\Delta}_n(\lambda)$  are defined by

$$\begin{aligned} x_n(\lambda) &= \sqrt{2U\Gamma} \operatorname{Re} \left( \lambda + i\frac{n}{2} \right)^{1/2} + n\left(\frac{U}{2} + \epsilon_d\right) \\ \tilde{\Delta}_n(\lambda) &= -\frac{1}{\pi} \partial_\lambda \delta_n(\lambda) \\ &\equiv -\frac{1}{\pi} \partial_\lambda \operatorname{Re} \delta(-\sqrt{2U\Gamma} (\lambda + i\frac{n}{2})^{1/2} + U/2 + \epsilon_d) \\ &\quad -\frac{1}{2\pi} \partial_\lambda \sum_{k=1}^{n-1} \left\{ \delta(-\sqrt{2U\Gamma} (\lambda + \frac{i}{2}(n-2k))^{1/2} + U/2 + \epsilon_d) \right. \\ &\quad \left. + \delta(\sqrt{2U\Gamma} (\lambda + \frac{i}{2}(n-2k))^{1/2} + U/2 + \epsilon_d) \right\}. \end{aligned} \quad (2.25)$$

The kernels in the above density integral equations are

$$\begin{aligned} a_n(\lambda) &= \frac{2n}{\pi} \frac{1}{(n^2 + 4\lambda^2)}; \\ A_{nm}(\lambda) &= \delta_{nm} \delta(\lambda) + a_{|n-m|}(\lambda) \\ &\quad + 2 \sum_{k=1}^{\min(n,m)-1} a_{|n-m|+2k}(\lambda) + a_{n+m}(\lambda). \end{aligned} \quad (2.26)$$

In the above,  $\rho_{p/h}(q)$  describe the particle/hole occupancy of the real  $q$ -excitations. The total density of states,  $\rho(q)$ , is equal to the sum of the two

$$\rho(q) = \rho_p(q) + \rho_h(q).$$

To compare with the  $T = 0$  density equations, we note that at  $T = 0$ ,

$$\begin{aligned} \rho_p(q) &= \Theta(B - q) \rho(q); \\ \rho_h(q) &= \Theta(q - B) \rho(q). \end{aligned}$$

$\sigma_{p/hn}(\lambda)$  similarly describe the finite temperature particle/hole occupancies of the  $n$ -spin complexes with associated complex  $q$ 's (here  $\lambda$  refers to the string centre). At  $T = 0$  we have for comparison

$$\begin{aligned} \sigma_{pn}(\lambda) &= 0, n > 1; \\ \sigma_{p1}(\lambda) &= \sigma_1(\lambda) \Theta(\lambda - Q); \\ \sigma_{h1}(\lambda) &= \sigma_1(\lambda) \Theta(Q - \lambda). \end{aligned} \quad (2.27)$$

Finally  $\sigma'_{p/hn}(\lambda)$  describes the particle/hole densities of the  $n$ -spin complexes without associated complex- $q$ 's. At  $T = 0$ ,  $\sigma'_{pn}(\lambda)$  are uniformly zero (none of these excitations appear in the ground state).

The energies of creating the various types of excitations are indifferent to the form of the impurity scattering phase (as at  $T = 0$  in Eqn. (2.21)). Thus these energies are the same as for the single dot case (see Ref. (36)) and are given by

$$\epsilon_q(q) = q$$

$$\begin{aligned} &+ T \sum_{n=1}^{\infty} \int_{-\infty}^{\infty} d\lambda \log\left(\frac{f(-\epsilon'_{\lambda n}(\lambda))}{f(-\epsilon_{\lambda n}(\lambda))}\right) a_n(\lambda - g(q)); \\ \log(f(\epsilon_{\lambda n}(\lambda))) &= -\frac{2}{T} x_n(\lambda) \\ &- \int_{-\infty}^{\infty} dq g'(q) \log(f(-\epsilon_q(q))) a_n(g(q) - \lambda) \\ &+ \sum_{m=1}^{\infty} \int d\lambda' A_{nm}(\lambda - \lambda') \log(f(-\epsilon_{\lambda m}(\lambda'))); \\ \log(f(\epsilon'_{\lambda n}(\lambda))) &= \\ &- \int_{-\infty}^{\infty} dq g'(q) \log(f(-\epsilon_q(q))) a_n(g(q) - \lambda) \\ &+ \sum_{m=1}^{\infty} \int d\lambda' A_{nm}(\lambda - \lambda') \log(f(-\epsilon'_{\lambda m}(\lambda'))), \end{aligned} \quad (2.28)$$

where  $f(\epsilon) = (1 + \exp(\epsilon/T))^{-1}$  is the Fermi distribution. These energies are related to the various particle-hole densities via

$$\begin{aligned} \rho_{p/h}(q) &= (\rho_p(q) + \rho_h(q)) f(\pm \epsilon_q(q)) \equiv \rho(q) f(\pm \epsilon(q)); \\ \sigma_{p/hn}(\lambda) &= (\sigma_{pn}(\lambda) + \sigma_{hn}(\lambda)) f(\pm \epsilon_{\lambda n}(\lambda)) \\ &\equiv \sigma(\lambda) f(\pm \epsilon_{\lambda n}(\lambda)); \\ \sigma'_{p/hn}(\lambda) &= (\sigma'_{pn}(\lambda) + \sigma'_{hn}(\lambda)) f(\pm \epsilon'_{\lambda n}(\lambda)) \\ &\equiv \sigma'(\lambda) f(\pm \epsilon'_{\lambda n}(\lambda)); \end{aligned} \quad (2.29)$$

These equations are arrived at from minimizing the free energy of the system. The solutions to Eqns. (2.24) and (2.28) represent the distribution of excitations in thermal equilibrium.

### III. COMPUTING TRANSPORT PROPERTIES: METHODOLOGY

Here we describe how to extract the scattering phases of electrons off the dot system from the Bethe ansatz equations. We do so both for the system at zero and finite temperature *in equilibrium*. We believe that the results are obtained by this methodology are *exact* at  $T = 0$  and an *excellent approximation* at finite  $T$ . The nature of this finite  $T$  approximation is discussed in detail in Ref. (36).

#### A. General Considerations

To compute transport properties we must translate the effects of the map between the  $L/R$  and the even/odd electrons. Excitations in the even/odd picture scatter off the collection of dots with some pure scattering phase,  $\delta_{e/o}(E)$ , where  $E$  is the energy of the excitation. This is true regardless of energy as there are no inelastic processes to take into account. The excitations are exact

eigenstates of the system and not merely asymptotic approximations. The transmission/reflection (T/R) amplitudes of an excitation in the  $L/R$  basis are related to the two scattering phases,  $\delta_{e/o}$  via the following ansatz:

$$\begin{aligned} e^{i\delta_e(E)} &= \mathcal{R}(E) + \mathcal{T}(E); \\ e^{i\delta_o(E)} &= 1 = \mathcal{R}(E) - \mathcal{T}(E). \end{aligned} \quad (3.1)$$

$\delta_o(E)$  is necessarily 0 as the odd sector is uncoupled from the dots.

The computation of the  $\delta_e(E)$  for a given excitation is described in detail in Ref. (36). It is based on a technique used to compute the magnetoresistance in the Kondo model.<sup>42</sup> The scattering phase is identified with the portion of an excitation's momentum scaling as  $1/L$ :

$$p = p^{\text{bulk}} + p^{\text{imp}}/L = p^{\text{bulk}} + \delta_e(E)/L. \quad (3.2)$$

For the purposes of computing transport properties, we are interested in the scattering of electronic excitations. In the Bethe ansatz solution of this model, all excitations see a spin-charge separation. In order to construct an electronic excitation, we must glue together a charge excitation with a spin excitation. How this is done and potential (finite energy/temperature) pitfalls are again discussed in detail in Ref. (36). A spin  $\uparrow$  electron can be treated as a composite of a right-moving real  $q$ -excitation and a left moving  $\lambda$ -hole (here by a  $\lambda$ -hole we mean a hole in a 1-spin complex with associated complex  $q$ 's). Thus

$$\delta_{\text{electron}\uparrow} = p_q^{\text{imp}}(q) + p_\lambda^{\text{imp}}(\lambda). \quad (3.3)$$

The energy of this composite particle is

$$\epsilon_{\text{el}} = \epsilon_q(q) - \epsilon_\lambda(\lambda). \quad (3.4)$$

The scattering of spin  $\downarrow$  electrons can be accessed through a particle-hole transformation.

## B. Zero Temperature

At  $T = 0$ , we are interested in zero energy excitations at the Fermi surface. The conductance through the dot is given by:

$$\begin{aligned} G &= \frac{e^2}{h} (|T_\uparrow(E=0)|^2 + |T_\downarrow(E=0)|^2) \\ &= \frac{e^2}{h} \left( \sin^2\left(\frac{\delta_{e\uparrow}(E=0)}{2}\right) + \sin^2\left(\frac{\delta_{e\downarrow}(E=0)}{2}\right) \right). \end{aligned} \quad (3.5)$$

The zero energy composite excitation is constructed by choosing the  $q$ -,  $\lambda$ -excitations at their Fermi surfaces  $q = B/\lambda = Q$ . (At zero temperature  $\epsilon_q(q = B) = \epsilon_\lambda(\lambda = Q) = 0$ .)

A simplification in the computation of scattering phases arises from a relationship between the impurity

momenta and the impurity densities. The impurity density is simply the portion of the density scaling as  $1/L$ , that is, the piece sensitive to the presence of the dots:

$$\begin{aligned} \rho(q) &= \rho_{\text{bulk}}(q) + \rho^{\text{imp}}(q); \\ \sigma(\lambda) &= \sigma_{\text{bulk}}(\lambda) + \sigma^{\text{imp}}(\lambda). \end{aligned} \quad (3.6)$$

Thus  $\rho^{\text{imp}}(q)$  and  $\sigma^{\text{imp}}(\lambda)$  satisfy

$$\begin{aligned} \rho^{\text{imp}}(q) &= \Delta(q) + g'(q) \int_Q^{\tilde{Q}} d\lambda a_1(g(q) - \lambda) \sigma^{\text{imp}}(\lambda); \\ \sigma^{\text{imp}}(\lambda) &= \tilde{\Delta}(\lambda) - \int_Q^{\tilde{Q}} d\lambda' a_2(\lambda' - \lambda) \sigma^{\text{imp}}(\lambda') \\ &\quad - \int_{-D}^B dq a_1(\lambda - g(q)) \rho^{\text{imp}}(q), \end{aligned} \quad (3.7)$$

In Ref. (36), it is then shown that

$$\partial_q p_q^{\text{imp}}(q) = 2\pi \rho^{\text{imp}}(q); \quad \partial_\lambda p_\lambda^{\text{imp}}(\lambda) = -2\pi \sigma^{\text{imp}}(\lambda). \quad (3.8)$$

Thus by computing the impurity densities we can access the scattering phases of the excitations. In particular we see

$$\begin{aligned} p_q^{\text{imp}}(B) &= 2\pi \int_{-D}^B dq \rho^{\text{imp}}(q); \\ p_\lambda^{\text{imp}}(Q) &= 2\pi \int_Q^{\tilde{Q}} d\lambda \sigma^{\text{imp}}(\lambda). \end{aligned} \quad (3.9)$$

We point out that the integrated densities do not necessarily equal the number of electrons sitting on the dots. For example

$$\sum_i n_{\uparrow i} + n_{\downarrow i} \neq \int_{-D}^B dq \rho^{\text{imp}}(q) + \int_Q^{\tilde{Q}} d\lambda \sigma^{\text{imp}}(\lambda),$$

as would be the case for a single dot. Rather the r.h.s. of the above equation includes contributions coming from  $1/L$  changes in the electron density of the leads. We will discuss this further in Sections V and VII.

## C. Finite Temperature

At finite temperature, the calculation is less straightforward. We must both take into account all the thermally excited excitations and their dressing of the electron scattering phase.<sup>36</sup> For a variety of technical reasons, this is only feasible at the symmetric point of the dots, i.e.  $U_{ii}/2 + \epsilon_{di} = 0$  as explained in Ref. (36). At finite  $T$  the electronic excitations have a Fermi distribution and so the conductance,  $G$ , equals

$$G = \frac{e^2}{h} \int dE \left( -\frac{\partial f}{\partial E} \right) (|T_\uparrow(E)|^2 + |T_\downarrow(E)|^2). \quad (3.10)$$

To determine the scattering probabilities,  $T_{\uparrow/\downarrow}(E) = \sin^2(\frac{\delta(E,T)}{2})$ , we construct excitations above the thermal ground state discussed in Section II.B.2 in analogy to what we did at  $T = 0$ . The electronic excitations are built out of real  $q$  and an  $n = 1$  spin-charge complex,  $\lambda$  (in the language of Section II.B.2). We have specifically

$$\delta_{el\uparrow}(\epsilon = \epsilon_{el}, T) = p_q^{\text{imp}}(q) + p_{1\lambda}^{\text{imp}}(\lambda). \quad (3.11)$$

However here  $p_q^{\text{imp}}(q)$  and  $p_{1\lambda}^{\text{imp}}(\lambda)$  are dressed by the presence of the other thermal excitations in the ground state. The finite temperature form of  $p^{\text{imp}}(q)$  and  $p_{1\lambda}^{\text{imp}}(\lambda)$  is:<sup>36</sup>

$$\begin{aligned} p_q^{\text{imp}}(q) &= \delta(q) + \sum_{n=1}^{\infty} \int_{-\infty}^{\infty} \theta_n(g(q) - \lambda) \\ &\quad \times (\sigma_{pn}^{\text{imp}}(\lambda) + \sigma'_{pn}{}^{\text{imp}}(\lambda)); \\ p_{1\lambda}^{\text{imp}}(\lambda) &= 2\delta_1(\lambda) + \int_{-\infty}^{\infty} dq \rho_p^{\text{imp}}(q) \theta_1(\lambda - g(q)) \\ &\quad + \sum_{m=1}^{\infty} \int d\lambda' \Sigma_{1m}(\lambda - \lambda') \sigma_{pm}^{\text{imp}}(\lambda'), \end{aligned} \quad (3.12)$$

where the kernels  $\theta_n(\lambda)$  and  $\sigma_{1m}(\lambda)$  are given by

$$\begin{aligned} \theta_n(\lambda) &= 2 \tan^{-1}\left(\frac{2}{n}\lambda\right) - \pi; \\ \Sigma_{nm}(\lambda) &= \theta_{|n-m|}(\lambda) \\ &\quad + 2 \sum_{k=1}^{\min(n,m)-1} \theta_{|n-m|+2k}(\lambda) + \theta_{n+m}(\lambda). \end{aligned} \quad (3.13)$$

Comparing the above with Eqn. (2.25), we find the relationship,

$$\begin{aligned} \partial_q p_q^{\text{imp}}(q, T) &= 2\pi \rho^{\text{imp}}(q, T); \\ \partial_\lambda p_{1\lambda}^{\text{imp}}(\lambda, T) &= -2\pi \sigma_1^{\text{imp}}(q, T) \end{aligned} \quad (3.14)$$

Hence at finite temperature

$$\begin{aligned} \delta_{el\uparrow}(T) &= 2\pi \int_{-D}^q dq \rho^{\text{imp}}(q, T) \\ &\quad + 2\pi \int_{\lambda}^{\tilde{Q}} d\lambda \sigma_1^{\text{imp}}(\lambda, T), \end{aligned} \quad (3.15)$$

a generalization of Eqns. (3.3) and (3.9).

We need to determine how to choose  $q$  and  $\lambda$  at finite temperature. If we are interested in constructing an excitation of energy,  $\epsilon_{el}$ , out of a  $q$ -particle and a  $\lambda$ -hole we must insist that

$$\epsilon_{el} = \epsilon_q(q) - \epsilon(\lambda). \quad (3.16)$$

This would seem to provide a two parameter space  $(q, \lambda)$  for characterizing excitations. However as explained in Ref. (36), we fix  $\lambda$  to some value  $\lambda_0$  allowing only  $q$  to

vary. One justification for doing so lies in the nature of the physics at the symmetric point. At the symmetric point, Kondo physics will be present in some form governed by a scale,  $T_K$ . Of the two energies only  $\epsilon(q)$  sees variations on this scale.  $\epsilon(\lambda)$  in contrast see variations on the much larger energy scale,  $\sqrt{U_{ii}\Gamma_i}$  governing charge fluctuations. Thus it is natural to only vary  $q$ . To fix  $\lambda_0$  we exploit the fact that at the symmetric point of the dot system, we expect the scattering phase to similarly symmetric about zero energy, i.e.

$$\delta_{el}(\epsilon, T) = \delta_{el}(-\epsilon, T). \quad (3.17)$$

We thus have

$$\begin{aligned} \delta_{el\uparrow}(\epsilon_{el}, T) &= 2\pi \int_{-D}^q dq \rho^{\text{imp}}(q, T) \\ &\quad + 2\pi \int_{\lambda_0}^{\tilde{Q}} d\lambda \sigma_1^{\text{imp}}(\lambda, T), \end{aligned} \quad (3.18)$$

with  $q$  chosen such than

$$\epsilon_{el} = \epsilon(q) - \epsilon(\lambda_0). \quad (3.19)$$

To compute  $\delta_{e\uparrow}$  from Eqn. (3.18), we need to compute  $\rho^{\text{imp}}(q)$  and  $\sigma_1^{\text{imp}}(\lambda)$ . This can be done by solving Eqns. (2.24) and (2.28). However at the symmetric point and at energies much smaller than  $\sqrt{U_{ii}\Gamma_i}$ , these equations can be simplified. If we recast the energies as

$$\begin{aligned} \phi_n(\lambda) &= \frac{1}{T} \epsilon_n(\lambda - \frac{1}{\pi} \log(\frac{2A}{T})); \\ \phi'_1(g(q)) &= -\frac{1}{T} \epsilon(-g(q) + \frac{1}{\pi} \log(\frac{2A}{T})); \\ \phi'_{n+1}(\lambda) &= \frac{1}{T} \epsilon'_n(-\lambda + \frac{1}{\pi} \log(\frac{2A}{T})); \\ A &= \frac{\sqrt{2U\Gamma}}{2\pi}, \end{aligned} \quad (3.20)$$

we can show that they satisfy the following set of integral equations

$$\begin{aligned} \xi_n(\lambda) &= -\int_{-\infty}^{\infty} d\lambda' s(\lambda - \lambda') \log(f(T\xi_{n-1}(\lambda))f(T\xi_{n+1}(\lambda))) \\ &\quad - \delta_{n1} e^{\pi\lambda}, \end{aligned} \quad (3.21)$$

where  $\xi_n = \phi_n$  or  $\phi'_n$  and  $s(\lambda) = \cosh^{-1}(\pi\lambda)/2$ .

The impurity density equations take the initial form given in Eqn. (2.24). If we focus upon energies  $\ll \sqrt{U_{ii}\Gamma_i}$ , we can safely assume

$$\sigma_{h1}^{\text{imp}}(\lambda) = 0; \quad \sigma_m^{\text{imp}} = 0; \quad m > 1. \quad (3.22)$$

The impurity densities then reduce to

$$\begin{aligned} \rho^{\text{imp}}(q) &= \Delta(q) \\ &\quad + g'(q) \sum_{n=1}^{\infty} \int_{-\infty}^{\infty} d\lambda a_n(g(q) - \lambda) \sigma'_{pn}{}^{\text{imp}}(\lambda); \end{aligned}$$

$$\begin{aligned}
& +g'(q) \int_{-\infty}^{\infty} d\lambda a_1(g(q) - \lambda) \sigma_{p1}^{\text{imp}}(\lambda); \\
\sigma_{h1}^{\text{imp}}(\lambda) &= \tilde{\Delta}_1(\lambda) - \int_{-\infty}^{\infty} dq \rho_p^{\text{imp}}(q) a_1(\lambda - g(q)) \\
& - \int_{-\infty}^{\infty} d\lambda' a_2(\lambda - \lambda') \sigma_{p1}^{\text{imp}}(\lambda'); \\
\sigma_{hn}^{\text{imp}}(\lambda) &= \int_{-\infty}^{\infty} dq \rho_p^{\text{imp}}(q) a_n(\lambda - g(q)) \\
& - \int_{-\infty}^{\infty} d\lambda' \sum_{m=1}^{\infty} A_{nm}(\lambda - \lambda') \sigma_{pm}^{\text{imp}}(\lambda'). \quad (3.23)
\end{aligned}$$

Using the inverse of the matrix  $A_{nm}$ ,

$$A_{nm}^{-1}(\lambda) = \delta_{nm} \delta(\lambda) - s(\lambda)(\delta_{nm+1} + \delta_{nm-1}), \quad (3.24)$$

together with the relationship

$$\delta_{n1} s(\lambda - \lambda'') = \int_{-\infty}^{\infty} d\lambda' A_{nm}^{-1}(\lambda - \lambda') a_m(\lambda' - \lambda''), \quad (3.25)$$

we obtain

$$\begin{aligned}
\rho^{\text{imp}}(q) &= \Delta(q) + g'(q) \int_{-\infty}^{\infty} d\lambda s(\lambda - g(q)) \tilde{\Delta}_1(\lambda) \\
& - g'(q) \int_{-\infty}^{\infty} d\lambda s(\lambda - g(q)) \sigma_{h1}^{\text{imp}}(\lambda); \\
\sigma_{p1}^{\text{imp}}(\lambda) + \sigma_{h1}^{\text{imp}}(\lambda) &= - \int_{-\infty}^{\infty} d\lambda' R(\lambda - \lambda') \tilde{\Delta}_1(\lambda') \\
& + \tilde{\Delta}_1(\lambda') - \int_{-\infty}^{\infty} dq \rho_h^{\text{imp}}(q) s(\lambda - g(q)); \\
\sigma_{pn}^{\text{imp}}(\lambda) + \sigma_{hn}^{\text{imp}}(\lambda) &= \delta_{n1} \int_{-\infty}^{\infty} dq \rho_p^{\text{imp}}(q) s(\lambda - g(q)) \\
& + \int_{-\infty}^{\infty} d\lambda' s(\lambda - \lambda') (\sigma_{hn+1}^{\text{imp}}(\lambda') + \sigma_{hn-1}^{\text{imp}}(\lambda')) \quad (3.26)
\end{aligned}$$

In this form, the equations are easily solved numerically through iteration.

This computation of the finite temperature conductance comes with some potential pitfalls as discussed in Ref. (36). However as shown in this same reference we are able to accurately reproduce the universal finite temperature linear response conductance scaling curve for a single dot. Uncertainties arose with the application of this methodology because of uncertainties with identifying the correct bulk scattering states. Here however the choice of bulk scattering states is exactly the same – differences between the treatment here and Ref. (36) only arise at the level of impurity scattering. As our choice of bulk scattering states was unproblematic previously, we expect it to be similarly so here.

#### IV. ANALYSIS OF EQUATIONS GOVERNING ZERO TEMPERATURE TRANSPORT OF DOUBLE DOTS IN PARALLEL

In this section we will analyze in detail the equations governing zero temperature transport in double quantum dots. As discussed in Section II.B, there are two sets of constraints under which a pair of dots in parallel is integrable. The most interesting set of constraints is given in Eqn. (2.8):

$$U_{\alpha\alpha'} = \delta_{\alpha\alpha'} U_{\alpha}; \quad U_{\alpha} \Gamma_{\alpha} = U_{\alpha'} \Gamma_{\alpha'};$$

$$U_{\alpha} + 2\epsilon_{d\alpha} = U_{\alpha'} + 2\epsilon_{d\alpha'}; \quad (4.1)$$

These conditions correspond to well separated parallel dots. They are neither capacitively nor tunneled coupled. The second set of conditions, corresponding to the constraints,

$$U_{\alpha\alpha'} = U; \quad \Gamma_{\alpha} = \Gamma_{\alpha'}; \quad \epsilon_{\alpha} = \epsilon_{\alpha'}, \quad (4.2)$$

leads to transport that is identical in nature to a single level dot. As such we will focus primarily in this section on parallel dots meeting the first set of constraints and only briefly discuss dots constrained by the second set at the section's end.

At zero temperature, as discussed in Section III.A, the scattering phases which determines the transport are expressed in terms of the two impurity densities,  $\rho^{\text{imp}}(q)$  and  $\sigma^{\text{imp}}(\lambda)$ . These two densities satisfy the two integral equations (Eqn. (3.7)):

$$\begin{aligned}
\rho^{\text{imp}}(q) &= \rho_0^{\text{imp}}(q) + g'(q) \int_Q^{\tilde{Q}} d\lambda a_1(g(q) - \lambda) \sigma^{\text{imp}}(\lambda); \\
\sigma^{\text{imp}}(\lambda) &= \sigma_0^{\text{imp}}(\lambda) - \int_Q^{\tilde{Q}} d\lambda' a_2(\lambda' - \lambda) \sigma^{\text{imp}}(\lambda') \\
& - \int_{-D}^B dq a_1(\lambda - g(q)) \rho^{\text{imp}}(q). \quad (4.3)
\end{aligned}$$

The ‘Fermi surfaces’ of the dots,  $Q$  and  $B$  are determined by the conditions given in Eqn. (2.19). As  $Q$  and  $B$  (up to  $1/L$  corrections) are given solely by the bulk densities  $\sigma^{\text{bulk}}(\lambda)$  and  $\rho^{\text{bulk}}(q)$ , their behaviour, as a function of the two quantities  $2\epsilon_{d1/2} - U_{11/22}$  and  $\Gamma_{1/2} U_{11/22}$ , is exactly the same as that of a single level dot and so discussed extensively in Refs.(35) and (36).

The equations in Eqn. (4.3) can only be solved in general numerically. However they do admit analytic solutions in certain cases in two limits: a)  $|\epsilon_{d1} - \epsilon_{d2}| \gg \Gamma_1, \Gamma_2$  and b)  $|\epsilon_{d1} - \epsilon_{d2}| \ll \Gamma_1, \Gamma_2$ . In both cases the source terms,  $\rho_0^{\text{imp}}(q)$  and  $\sigma_0^{\text{imp}}(\lambda)$  can be written in the form

$$\begin{aligned}
\rho_0^{\text{imp}}(q) &\approx \Delta_{01}^{\text{imp}}(q) + \Delta_{02}^{\text{imp}}(q); \\
\sigma_0^{\text{imp}}(\lambda) &\approx \sigma_{01}^{\text{imp}}(\lambda) + \sigma_{02}^{\text{imp}}(\lambda), \quad (4.4)
\end{aligned}$$

where

$$\Delta_{0i}^{\text{imp}}(q) = \frac{\tilde{\Gamma}_i}{\tilde{\Gamma}_i^2 + (q - \tilde{\epsilon}_{di})^2};$$

$$\begin{aligned}
\sigma_{0i}^{\text{imp}}(\lambda) &= -\text{Re} \frac{1}{\pi} \partial_\lambda \Delta_{0i}(x(\lambda) + iy(\lambda)); \\
&= \int_{-\infty}^{\infty} dq \Delta_{0i}(q) a_1(\lambda - g(q)) \\
&\quad - a_1(\lambda - g(\tilde{\epsilon}_{di} + i\tilde{\Gamma}_i)) + \beta_i a_1(\beta_i \lambda - \gamma_i); \\
\alpha_i &= \frac{U_i}{2} + \epsilon_{di} - \tilde{\epsilon}_{di}; \\
\beta_i &= \frac{U_i \Gamma_i}{2\alpha_i \tilde{\Gamma}_i}.
\end{aligned} \tag{4.5}$$

The parameters  $\tilde{\epsilon}_{di}$  and  $\tilde{\Gamma}_i$  are case dependent. For case a), we obtain:

$$|\epsilon_{d1} - \epsilon_{d2}| \gg \Gamma_1, \Gamma_2 :$$

$$\begin{aligned}
\tilde{\Gamma}_{1/2} &= \Gamma_{1/2} + \frac{\Gamma_1 \Gamma_2}{(\epsilon_{d1} - \epsilon_{d2})^2} (\Gamma_{1/2} - \Gamma_{2/1}); \\
\tilde{\epsilon}_{d1/2} &= \epsilon_{d1/2} - \frac{\Gamma_1 \Gamma_2}{\epsilon_{d1/2} - \epsilon_{d2/1}},
\end{aligned} \tag{4.6}$$

and for case b)

$$|\epsilon_{d1} - \epsilon_{d2}| \ll \Gamma_1, \Gamma_2 :$$

$$\begin{aligned}
\tilde{\Gamma}_1 &= \Gamma_1 + \Gamma_2; \\
\tilde{\epsilon}_{d1} &= \frac{\epsilon_{d1} + \epsilon_{d2}}{2}; \\
\tilde{\Gamma}_2 &= \frac{(\epsilon_{d1} - \epsilon_{d2})^2 \Gamma_1 \Gamma_2}{(\Gamma_1 + \Gamma_2)^3}; \\
\tilde{\epsilon}_{d2} &= \epsilon_{d2} + (\epsilon_{d1} - \epsilon_{d2}) \frac{\Gamma_2}{\Gamma_1 + \Gamma_2}.
\end{aligned} \tag{4.7}$$

If  $\epsilon_{d1} = \epsilon_{d2}$  exactly, then  $\tilde{\Gamma}_2$  vanishes and  $\Delta_{02}(q)$  is identically zero.

Given the division of the source terms into two pieces and the linearity of the equations in (4.3), we can correspondingly write  $\sigma(\lambda) = \sigma_1(\lambda) + \sigma_2(\lambda)$  and  $\rho(\lambda) = \rho_1(\lambda) + \rho_2(\lambda)$  where

$$\begin{aligned}
\rho_i^{\text{imp}}(q) &= \rho_{0i}^{\text{imp}}(q) + g'(q) \int_Q^{\tilde{Q}} d\lambda a_1(g(q) - \lambda) \sigma_i^{\text{imp}}(\lambda); \\
\sigma_i^{\text{imp}}(\lambda) &= \sigma_{0i}^{\text{imp}}(\lambda) - \int_Q^{\tilde{Q}} d\lambda' a_2(\lambda' - \lambda) \sigma_i^{\text{imp}}(\lambda') \\
&\quad - \int_{-D}^B dq a_1(\lambda - g(q)) \rho_i^{\text{imp}}(q),
\end{aligned} \tag{4.8}$$

#### A. Linear Response Conductance at Zero Magnetic Field

We compute the Fermi surface scattering phase,  $\delta_e$ , governing the linear response conductance,  $G = 2e^2/h \sin^2(\delta_e/2)$ , via

$$\delta_e = 2\pi \int_Q^\infty (\sigma_1^{\text{imp}} + \sigma_2^{\text{imp}})(\lambda)$$

$$\begin{aligned}
&= 2\pi - \pi \int_{-\infty}^Q (\sigma_1^{\text{imp}} + \sigma_2^{\text{imp}})(\lambda) \\
&= 2\pi - \delta_{e1} - \delta_{e2}.
\end{aligned} \tag{4.9}$$

The quantity,  $\int_Q^\infty$ , in first line of Eqn. (4.9) is the impurity particle number while the corresponding integrated quantity in the second line is the impurity hole number.  $\sigma_i^{\text{imp}}$  can be obtained via a Weiner-Hopf analysis of Eqn. (4.8) (with  $B = -D$ ). Our separation of the impurity densities into two pieces allows the computation to proceed along the lines of Ref. (35). We relegate the analysis to Appendix A simply reporting the results for  $\delta_{ei}$  below. These results apply to both  $\delta_{e1}$  and  $\delta_{e2}$  provided  $\epsilon_{d1} \neq \epsilon_{d2}$ . If instead  $\epsilon_{d1} = \epsilon_{d2}$ ,  $\delta_{e2}$  is identically zero and the equations below apply only to  $\delta_{e1}$ .

The analysis of  $\delta_{ei}$  breaks down into three cases depending on the value of  $Q$ , the parameter describing the position of the Fermi surface of the  $\lambda$ -excitations.

**Case i: Dots Near the Particle-Hole Symmetric Point**  $Q < 0$ : Near the symmetric point, i.e.  $U_i/2 + \epsilon_{di} \ll \sqrt{U\Gamma}$ , then  $Q < 0$ . Setting  $J_i \equiv I_i^{-1} - Q$ , where

$$I_i^{-1} = \frac{\alpha_i^2 - \tilde{\Gamma}_i^2}{2U_i \Gamma_i}, \tag{4.10}$$

$\delta_{ei}$  is then given by

$$\delta_{ei} = K_{i1} + K_{i2}. \tag{4.11}$$

Here  $K_{ij}$  is the contribution to the scattering phase,  $\delta_{ei}$ , coming from the bare impurity densities,  $\Delta_{0j}^{\text{imp}}(q)$  and  $\sigma_{0j}^{\text{imp}}(\lambda)$ . In this case we find (see Appendix A)

$$\begin{aligned}
K_{i1} &= \sqrt{\pi} \sum_{n=0}^{\infty} \frac{(-1)^n}{n+1/2} \left( \frac{n+1/2}{e} \right)^{n+1/2} \frac{1}{\Gamma(n+1)} \\
&\quad \times \int_{-\infty}^{\infty} dq \Delta_{0i}(q) e^{-\pi(2n+1)(g(q)-Q)}; \\
K_{i2} &= \text{sign}(1 - \beta_i) \sqrt{\pi} \mathbf{P} \int_0^{\infty} \frac{d\omega}{\omega} \left( \frac{\omega}{e} \right)^\omega \frac{e^{-2\pi\omega J_i}}{\Gamma(1/2 + \omega)} \\
&\quad \times \frac{\sin(2\pi\omega(\gamma_i - 1/2))}{\cos(\pi\omega)} \\
&\quad + \text{sign}(1 - \beta_i) \sqrt{\pi} \sum_{n=0}^{\infty} \frac{(-1)^n}{n+1/2} \left( \frac{n+1/2}{e} \right) \frac{e^{-(2n+1)\pi J_i}}{\Gamma(n+1)} \\
&\quad \times \cos(\pi(\gamma_i - 1/2)(2n+1)),
\end{aligned} \tag{4.12}$$

where  $\mathbf{P}$  indicates that the principal value of the integral is to be taken and  $\gamma_i = 1/2(1 - \beta_i^{-1})\text{sign}(1 - \beta_i)$ . The value of the Fermi surface,  $Q$ , was found in Refs. (35) and (36) to be determined implicitly by

$$\frac{2\epsilon_{di} + U_i}{\sqrt{2U_i \Gamma_i}} = \frac{\sqrt{2}}{\pi} \sum_{n=0}^{\infty} \frac{(-1)^n e^{\pi Q(2n+1)}}{(2n+1)^{3/2}} G^+(i\pi(2n+1)). \tag{4.13}$$

**Case ii: Mixed Valence Regime of the Dots:**  $Q > 0$  and  $J_i = I_i^{-1} - Q > 0$ : For these values of the parameters, we are in the mixed valence regime of the dots. Here  $\delta_{ei}$  is given by

$$\begin{aligned}\delta_{ei} &= K_{i1} + K_{i2} \\ K_{i1} &= \pi \left( \sqrt{2} - 1 - \frac{\pi}{\sqrt{26}} J_i + \pi^2 \frac{\sqrt{2}}{24^2} J_i^2 \right. \\ &\quad \left. + \frac{1}{\pi\sqrt{2}} (\beta_i^{-1} - 1) J_i + \mathcal{O}(J_i^3) + \mathcal{O}(J_i(\beta_i^{-1} - 1)) \right); \\ K_{i2} &= \text{sign}(1 - \beta_i) \sqrt{\pi} \mathbf{P} \int_0^\infty \frac{d\omega}{\omega} \left( \frac{\omega}{e} \right)^\omega \frac{e^{-2\pi\omega J_i}}{\Gamma(1/2 + \omega)} \\ &\quad \times \frac{\sin(2\pi\omega(\gamma_i - 1/2))}{\cos(\pi\omega)} \\ &\quad + \text{sign}(1 - \beta_i) \sqrt{\pi} \sum_{n=0}^\infty \frac{(-1)^n}{n + 1/2} \left( \frac{n + 1/2}{e} \right) \frac{e^{-(2n+1)\pi J_i}}{\Gamma(n + 1)} \\ &\quad \times \cos(\pi(\gamma_i - 1/2)(2n + 1)).\end{aligned}\quad (4.14)$$

If  $J_i$  is small,  $K_{i2}$  can be approximated by

$$K_{i2} = -\text{sign}(1 - \beta_i) \frac{\sqrt{2}}{\pi} \tan^{-1} \left( \frac{J_i}{\gamma_i} \right) \quad (4.15)$$

For  $\gamma_i$  small (as would be the case if  $|\epsilon_{d1} - \epsilon_{d2}| \ll \Gamma_{1,2}$ ) we see that  $K_{i2}$  undergoes a rapid variation as  $J_i$  is varied. This in turn will imply a rapid variation in both the  $T = 0$  linear response conductance and the number of localized electrons in the system as the gate voltage is swept.

In this case  $Q$  needs to be determined by a self-consistent numerical evaluation of Eqns. (2.23). If  $Q \sim 1$  however, it is a reasonable approximation to take

$$Q = q^* + \frac{1}{2\pi} \ln(2\pi e q^*), \quad (4.16)$$

where  $q^* = (\epsilon_{di} + U_i/2)^2 / (2U_i \Gamma_i)$ .

**Case iii: Empty orbital regime:**  $Q > 0$  and  $J_i = I_i^{-1} - Q < 0$ . In this parameter range, the dot filling is small.  $\delta_{ei}$  is then given by

$$\begin{aligned}\delta_{ei} &= K_{i1} + K_{i2} \\ K_{i1} &= \pi + \frac{1}{\sqrt{\pi}} \int_0^\infty \frac{d\omega}{\omega} \Gamma(1/2 + \omega) \left( \frac{e}{\omega} \right)^\omega e^{2\pi\omega J_i} \\ &\quad \times \sin(\pi\omega(1 + \frac{1}{\beta_i})); \\ K_{i2} &= \pi \text{sign}(1 - \beta_i) + \frac{1}{\sqrt{\pi}} \int_0^\infty \frac{d\omega}{\omega} \Gamma(1/2 + \omega) \\ &\quad \times \left( \frac{e}{\omega} \right)^\omega e^{2\pi\omega J_i} \sin(\pi\omega\gamma_i).\end{aligned}\quad (4.17)$$

If  $J_i$  is small, the expression for  $K_{i2}$  in Eqn. (4.15) holds equally well. Similarly, in this regime,  $Q$  is given as above in Eqn. (4.16).

## B. Finite Field Transport

In finite field, we must compute the scattering phases,  $\delta_{e\uparrow/\downarrow}$ , separately for spin up/down electrons. Like at  $H = 0$ , these scattering phases are given in terms of the impurity densities:

$$\begin{aligned}\delta_{e\uparrow} &= 2\pi \int_{-D}^B dq (\rho_1^{\text{imp}}(q) + \rho_2^{\text{imp}}(q)) \\ &\quad + 2\pi \int_Q^\infty (\sigma_1^{\text{imp}} + \sigma_2^{\text{imp}})(\lambda); \\ \delta_{e\downarrow} &= 2\pi \int_Q^\infty (\sigma_1^{\text{imp}} + \sigma_2^{\text{imp}})(\lambda).\end{aligned}\quad (4.18)$$

In general these equations cannot be solved analytically. However at the symmetric point they do admit such a solution. At this point,<sup>36</sup>  $Q = \infty$  and  $\sigma_i$  can be expressed solely in terms of  $\rho_i$  (simply by inverting Eqn. 4.8 via Fourier transform):

$$\begin{aligned}\sigma_i^{\text{imp}}(\lambda) &= \int_{-\infty}^\infty d\lambda' (1 + a_2)^{-1} (\lambda - \lambda') \sigma_{0i}^{\text{imp}}(\lambda') \\ &\quad - \int_{-D}^B dq \rho_i^{\text{imp}}(q) s(\lambda - g(q)).\end{aligned}\quad (4.19)$$

In turn, we obtain an equation for  $\rho_i^{\text{imp}}$  independent of  $\sigma_i^{\text{imp}}$ :

$$\rho_i^{\text{imp}}(q) = \rho_{0i}^{\text{imp}}(q) - g'(q) \int_{-\infty}^B dq' R(g(q) - g(q')) \rho^{\text{imp}}(q'), \quad (4.20)$$

where

$$R(\lambda) = \frac{1}{2\pi} \int_{-\infty}^\infty d\omega \frac{e^{-i\omega\lambda}}{1 + e^{|\omega|}}. \quad (4.21)$$

and we can write  $\rho_{0i}^{\text{imp}}(q)$  as

$$\begin{aligned}\rho_{0i}^{\text{imp}}(q) &= \Delta_{0i}(q) + g'(q) \int_{-\infty}^\infty dq R(g(q) - g(q')) \Delta_{0i}(q) \\ &\quad + \text{sign}(1 - \beta_i) g'(q) \int_{-\infty}^\infty \frac{d\omega}{2\pi} e^{-i\omega(g(q) - I_i^{-1})} \\ &\quad \times \frac{e^{\frac{|\omega|}{2}(1 - \beta_i^{-1}) \text{sign}(1 - \beta_i)}}{2 \cosh(\frac{\omega}{2})}.\end{aligned}\quad (4.22)$$

We are most interested in the behaviour of  $\rho_i^{\text{imp}}$  for  $q < 0$  as this is the region relevant for magnetotransport when  $H$  is on the order of the Kondo temperature. Following Ref. (35), for  $q < 0$  the first two terms may be rewritten as

$$\begin{aligned}\Delta_{0i}(q) + g'(q) \int_{-\infty}^\infty dq R(g(q) - g(q')) \Delta_{0i}(q) &= \\ -g'(q) \int_{-\infty}^\infty \frac{d\omega}{2\pi} \frac{e^{-i\omega(g(q) - I_i^{-1}) + \frac{|\omega|}{2} 1 - \beta^{-1}}}{2 \cosh(\frac{\omega}{2})}.\end{aligned}\quad (4.23)$$

At the symmetric point, the scattering phases similarly simplify reducing to

$$\begin{aligned}\delta_{e\uparrow} &= 2\pi + \pi \int_{-D}^B dq (\rho_1^{\text{imp}}(q) + \rho_2^{\text{imp}}(q)); \\ \delta_{e\downarrow} &= 2\pi - \pi \int_{-D}^B dq (\rho_1^{\text{imp}}(q) + \rho_2^{\text{imp}}(q)).\end{aligned}\quad (4.24)$$

We thus see that even though  $\delta_{e\uparrow}$  differs from  $\delta_{e\downarrow}$ , the conductance for each spin species is the same.

With the source term in this form, Eqn. (4.23) can be solved by a Wiener-Hopf analysis. We again relegate the details to Appendix A and here simply report the results. Firstly we consider the dependence of the limit  $B$ , the Fermi surface of the q-excitations, on the magnetic field. It has the same functional dependence on  $U_i + 2\epsilon_{di}$  and  $\Gamma_i U_i$  as in the case of a single level dot. Thus we can simply borrow results from Refs. (35) and (36):

$$\frac{H}{2\pi} = \left(\frac{U_i \Gamma_i}{8\pi^2}\right)^{1/2} \int_{-\infty}^{\infty} d\omega e^{-i\omega \frac{B^2}{2U_i \Gamma_i}} \frac{1}{(i\omega + \delta)^{1/2}} \frac{1}{\omega - i\delta}$$

$$\times \frac{1}{\Gamma(\frac{1}{2} + \frac{i\omega}{2\pi})} \left(\frac{i\omega + \delta}{2\pi e}\right)^{\frac{i\omega}{2\pi}}. \quad (4.25)$$

In the small  $H$  limit, one can deform the contour into the lower half plane, merely taking into account the pole nearest zero. We so obtain

$$b \equiv \frac{B^2}{2U_i \Gamma_i} = -\frac{1}{2\pi} \log \left( \frac{\pi e H^2}{4U\Gamma} \right). \quad (4.26)$$

Next we write down expressions for  $\int_{-D}^B dq \rho_i^{\text{imp}}(q)$ :

$$\int_{-D}^B dq \rho_i^{\text{imp}}(q) = S_i^{\text{Kondo}} + S_i^{\text{charge}}. \quad (4.27)$$

Here  $S_i^{\text{Kondo}}$  encodes information that varies on the Kondo scale. It is given by

$$S_i^{\text{Kondo}} = \begin{cases} \frac{2}{\sqrt{\pi}} \Theta(\beta_i - 1) \sum_{n=0}^{\infty} \frac{(-1)^n}{\Gamma(1+n)(n+\frac{1}{2})} \left( \frac{H\sqrt{\pi e}}{T_K^{\text{RKKY}} 2^{3/2}} \right)^{2n+1} \left( \frac{n+\frac{1}{2}}{e} \right)^{n+\frac{1}{2}} \cos(\pi(n+\frac{1}{2})(1-\beta_i^{-1})), & \text{if } b > I_i^{-1}, \\ 2\Theta(\beta_i - 1) \left[ 1 - \frac{1}{\pi^{3/2}} \int_0^{\infty} \frac{d\omega}{\omega} \left( \frac{8(T_K^{\text{RKKY}})^2}{\pi\omega H^2} \right)^{\omega} \Gamma(\frac{1}{2} + \omega) \sin(\pi\omega) \cos(\pi\omega(1-\beta_i^{-1})) \right], & \text{if } b < I_i^{-1}. \end{cases} \quad (4.28)$$

where the Kondo temperature is defined by

$$T_K^{\text{RKKY}} = \left( \frac{U_i \Gamma_i}{2} \right)^{1/2} e^{-\pi I_i^{-1}}, \quad \text{if } \beta_i > 1. \quad (4.29)$$

(We explain the label 'RKKY' in Section V.) This definition is well posed as of  $\beta_1$  and  $\beta_2$ , only one will be ever greater than 1. This Kondo temperature is similar to what is found in a single level dot but for the form of  $I_i^{-1}$  (see the definition in Eqn. (4.10) involving parameters renormalized by the effects of interference between the two dots). We can evaluate  $S_i^{\text{Kondo}}$  in the limit  $H \gg T_K^{\text{RKKY}}$  (but  $H < \sqrt{2U_i \Gamma_i / \pi e}$ ):

$$\begin{aligned} S_i^{\text{Kondo}} &= 2\Theta(\beta_i - 1) \left[ 1 - \frac{1}{2 \log(H/\tilde{T}_K^{\text{RKKY}})} \right. \\ &\quad + \mathcal{O}\left( \frac{\log \log(H/\tilde{T}_K^{\text{RKKY}})}{\log^2(H/\tilde{T}_K^{\text{RKKY}})} \right) + \frac{\pi^2(1-\beta_i^{-1})^2}{8 \log^3(H/\tilde{T}_K^{\text{RKKY}})} \\ &\quad + \mathcal{O}\left( \frac{(1-\beta_i^{-1})^2 \log \log(H/\tilde{T}_K^{\text{RKKY}})}{\log^4(H/\tilde{T}_K^{\text{RKKY}})} \right) \\ &\quad \left. + \mathcal{O}\left( \frac{(1-\beta_i^{-1})^4}{\log^5(H/\tilde{T}_K^{\text{RKKY}})} \right) \right], \end{aligned} \quad (4.30)$$

where  $\tilde{T}_K^{\text{RKKY}} = \frac{2^{3/2}}{\sqrt{\pi e}} T_K^{\text{RKKY}}$ . We have included the leading order term in  $(1-\beta_i^{-1})^2$  as this governs the differing

behaviour of  $S_i^{\text{Kondo}}$  in the two cases of  $|\epsilon_{d1} - \epsilon_{d2}| \ll \Gamma_{1,2}$  and  $|\epsilon_{d1} - \epsilon_{d2}| \gg \Gamma_{1,2}$ .

The second term,  $S_i^{\text{charge}}$ , varies on a scale comparable to the charging energy of the dot,  $\sqrt{U_i \Gamma_i}$ . In the dots' Kondo regime this scale will be much larger than  $T_K$ . It is given by

$$\begin{aligned} S_i^{\text{charge}} &= \frac{1}{\sqrt{\pi}} \sum_{n=0}^{\infty} \frac{e^{-2\pi b(n+\frac{1}{2})}}{\Gamma(1+n)(n+\frac{1}{2})} \left( \frac{n+\frac{1}{2}}{e} \right)^{n+\frac{1}{2}} \\ &\quad \times \int_{-\infty}^{\infty} dq e^{-2\pi g(q)(n+\frac{1}{2})} \Delta_{0i}(iq), \end{aligned} \quad (4.31)$$

and for fields  $H \sim T_K^{\text{RKKY}}$  makes a far smaller contribution than that of  $S_i^{\text{Kondo}}$ .

### C. Two degenerate dots in parallel

We now briefly consider two degenerate dots in parallel satisfying the conditions given in Eqn. (4.2). This case is less interesting than the one described by the conditions in Eqn. (4.1) as it is equivalent to a single level dot with Coulomb repulsion,  $U$ , and linewidth  $\Gamma = \sum_{\alpha} \Gamma_{\alpha}$ . This follows directly from Eqns. (2.4) and (2.15), the equations governing the bare impurity scattering phase,

$\delta(q)$ , and the function,  $g(q)$ , controlling the integrability of the dot model. Because  $U_{\alpha\alpha'} = U$  and  $\epsilon_{d\alpha} = \epsilon_d$ , we can make the replacement  $\Gamma \rightarrow \sum_{\alpha} \Gamma_{\alpha}$  and obtain equations corresponding to a single level dot.

With this equivalence, we can directly apply the analysis of the linear response conductance contained in Ref. (36). And so none of interesting phenomena identified in the coming two sections remains. In particular the RKKY Kondo effect, the presence of interference phenomena, and a non-trivial form of the Friedel sum rule are all absent.

## V. EXAMPLES OF ZERO TEMPERATURE TRANSPORT OF DOUBLE DOTS IN PARALLEL

In this section we consider various aspects of zero temperature transport in double quantum dots both in the absence and presence of a magnetic field. We will see that there is a mixture of different types of Kondo physics with interference effects. We will also see that the number of electrons displaced in attaching the quantum dots to the leads can be negative, a contrast to what is found in single level quantum dots. We begin by examining  $H = 0$  conductance of the dot system as a function of gate voltage.

### A. Zero Field Linear Response Conductance as a Function of Gate Voltage

Here we study the behaviour of the  $T = 0$  linear response conductance,  $G$ , as a function of gate voltage keeping the distance between the dot levels, i.e.  $|\epsilon_{d1} - \epsilon_{d2}|$ , fixed. Thus we allow the gate voltage to move the two dot chemical potentials in unison. In Figure 3 we plot four examples of  $G$  for dot systems with differing separations ranging from  $|\epsilon_{d1} - \epsilon_{d2}| \gg \Gamma_1, \Gamma_2$  to  $|\epsilon_{d1} - \epsilon_{d2}| = 0$ . Provided that  $|\epsilon_{d1} - \epsilon_{d2}| \neq 0$ , the conductance exhibits three basic features: i) an RKKY Kondo effect at the particle-hole symmetric point of the dot; ii) a standard Kondo effect corresponding to a value of gate voltage when one electron sits on the dot; and iii) interference effects whose strength is proportional to the separation of the two bare dot levels.

To understand this better let us begin by consider any of first three panels of Figure 3 (a, b, or c). Here  $|\epsilon_{d1} - \epsilon_{d2}|$  is nonzero. The linear response conductance trace begins at the particle hole symmetric point of the dot where (uniformly)  $\epsilon_{d1} = -10\Gamma_1$  and  $\epsilon_{d2} = -5\Gamma_1, -3\Gamma_1, -2\Gamma_1$  respectively for panels a), b), and c). At this point exactly two electrons sit on the two dot system. By the Friedel sum rule the corresponding scattering phase is  $\delta_e = 2\pi$  and the conductance vanishes. Although the conductance vanishes at this point, and counter to the intuition we have in a single level dot where Kondo physics is associated with a unitary maximum in the conductance, Kondo physics is still present. We determine its

presence by studying the low energy density of states of the impurity double dot system. We find what amounts to an Abrikosov-Suhl resonance.

In the Bethe ansatz language this amounts to studying the quantity  $\rho^{\text{imp}}(q(\epsilon))$  where  $\rho^{\text{imp}}(q)$  is the impurity density of states of the charge excitations and  $\epsilon_q(q)$  is their corresponding bulk excitation energy<sup>36,47</sup>. In zero magnetic field,  $\rho^{\text{imp}}(q)$  is equivalent to  $\rho_0^{\text{imp}}(q)$  computed in Appendix (A3):

$$\rho^{\text{imp}}(q < 0) = -2g'(q) \frac{\cos(\mu\pi) \cosh(\pi(g(q) - I_i^{-1}))}{\cosh(2\pi(g(q) - I_i^{-1})) + \cos(2\pi\mu)}. \quad (5.1)$$

where  $g(q) = (q - \epsilon_{di} - U_i/2)/(2U_i\Gamma_i)$  and  $\mu$  is given by

$$\mu = \begin{cases} \frac{1}{2}(1 - \beta_1^{-1}) & \text{if } \beta_1 > 1; \\ \frac{1}{2}(1 - \beta_2^{-1}) & \text{if } \beta_2 > 1, \end{cases} \quad (5.2)$$

where  $\beta_{1,2}$  are defined in Eqn. (4.5). Given the equivalence of the bulk equations between the single level dot and our two dots in parallel, the bulk energy of charge excitations,  $\epsilon_q(q)$ , can be taken from Refs. (35) and (36):

$$\epsilon_q(q) = \frac{\sqrt{2U_i\Gamma_i}}{\pi} e^{-\pi g(q)}. \quad (5.3)$$

This relationship is valid provided  $\epsilon_q(q)$  is on the order of the Kondo temperature. Substituting Eqn.(5.3) into Eqn. (5.1) we obtain the form of the Abrikosov-Suhl resonance of the dot system as a function of energy,  $\epsilon$ :

$$\rho^{\text{imp}}(\epsilon) = \frac{\cos(\pi\mu)}{T_K^{RKKY}} \frac{1 + \tilde{\epsilon}^2}{2\tilde{\epsilon}^2 \cos(2\pi\mu) + \tilde{\epsilon}^4 + 1}, \quad (5.4)$$

where  $\tilde{\epsilon} = \frac{\pi\epsilon}{2T_K^{RKKY}}$ . We plot the resonances for two cases,  $|\epsilon_{d1} - \epsilon_{d2}| \gg \Gamma_{1,2}$  and  $|\epsilon_{d1} - \epsilon_{d2}| \ll \Gamma_{1,2}$  in Figure 4. The plot is for positive energies (as the Bethe ansatz solution only directly gives positive energy information). However as we are at the particle-hole symmetric point the resonance itself will be symmetric about zero energy.

In the case  $|\epsilon_{d1} - \epsilon_{d2}| \gg \Gamma_{1,2}$ , i.e.  $\mu \sim 0$ , we obtain a resonance that has the familiar Lorentzian form associated with a single dot.<sup>36,47</sup> (see Figure 4). However this resonance has twice the integrated weight in comparison with a single dot. Thus even though  $|\epsilon_{d1} - \epsilon_{d2}| \gg \Gamma_{1,2}$ , we cannot think of this resonance as arising solely from Kondo physics involving the energetically lower of the two dot levels.

If  $0 < |\epsilon_{d1} - \epsilon_{d2}| \ll \Gamma_{1,2}$ , i.e.  $\mu \sim 1/2$ , the resonance dramatically changes structure. Instead of peaking at zero energy it has a sharp peak instead at  $\epsilon = 2T_K^{RKKY}/\pi$ . While the resonance does not vanish at zero energy in this case (inset to right panel of Figure 4), its value there is dramatically smaller than at  $\epsilon = 2T_K^{RKKY}/\pi$  (by a factor of  $1/4 \cos^2(\pi\mu)$ ). The resonance has thus split about zero energy. This splitting is akin to the splitting seen in the Kondo resonance when an interdot tunneling term,  $d_1^\dagger d_2 + d_2^\dagger d_1$ , is turned on between two degenerate dots, i.e.  $\epsilon_{d1} = \epsilon_{d2}$ .<sup>17,18,26</sup> However unlike this case the splitting is not proportional to

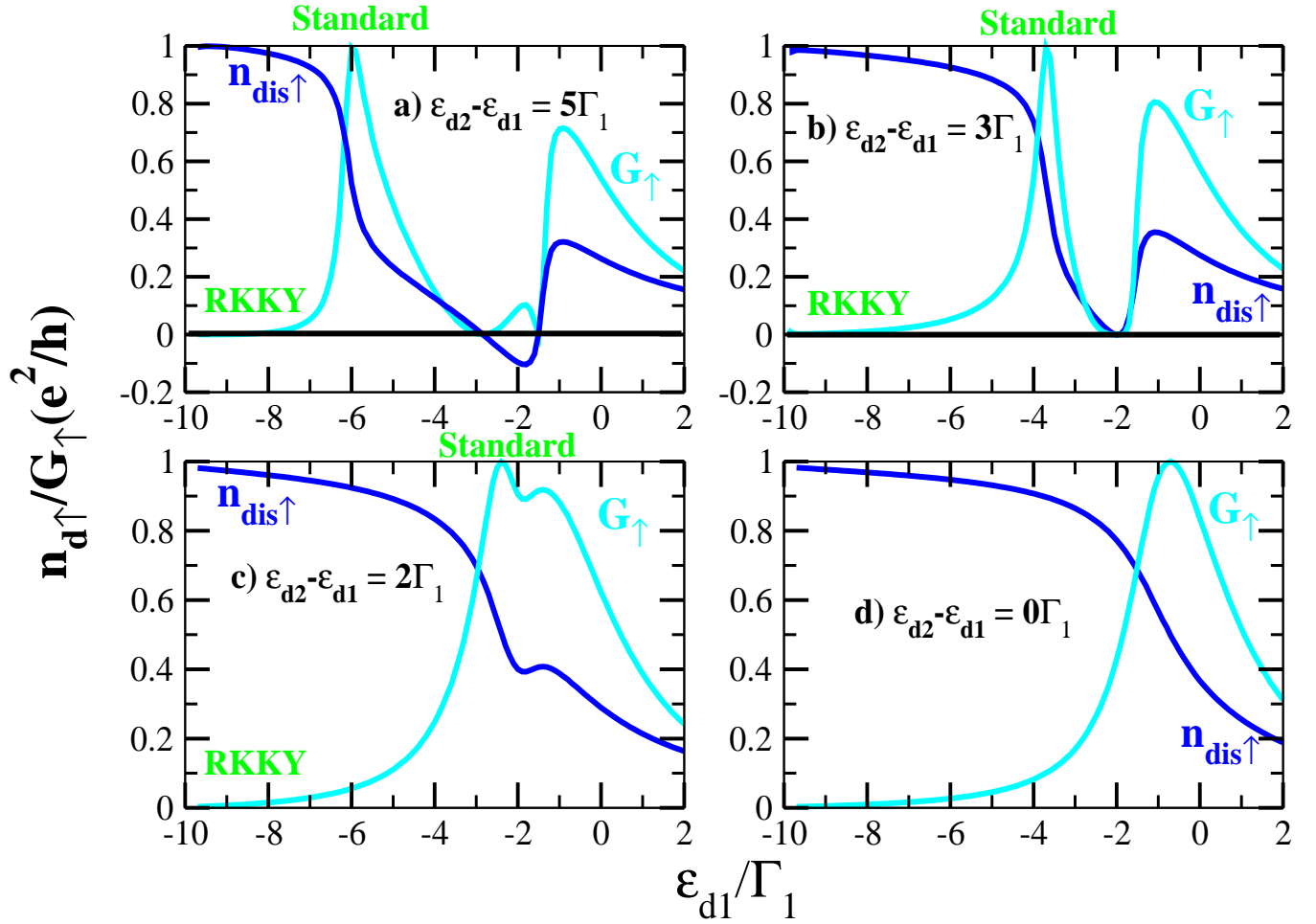


FIG. 3: Plots of the  $T=0$   $H=0$  linear response conductance as a function of gate voltage. In making these plots, we chose  $U_1 = 1$  and  $\Gamma_1 = U_1/20$  uniformly and values of  $|\epsilon_{d1} - \epsilon_{d2}|$  to be  $5\Gamma_1$ ,  $3\Gamma_1$ ,  $2\Gamma_1$  and  $0$  in panels a, b, c, and d.  $\Gamma_2$  and  $U_2$  are then chosen in accordance with the integrability conditions of Eqn. (2.8). On the plots we mark the values of gate voltage where the RKKY Kondo effect and the standard Kondo effect take place.

the bare scale  $|\epsilon_{d1} - \epsilon_{d2}|$ , but rather to the much smaller dynamical scale,  $T_K^{\text{RKKY}}$ .

A note of caution is in order. What we have just computed is the low energy density of states due the impurity double dot. But it is not exactly equivalent to the impurity Green's function

$$\langle d_1^\dagger d_1 \rangle_{\text{ret}}(\omega) + \langle d_2^\dagger d_2 \rangle_{\text{ret}}(\omega)$$

Formally the two differ by energy dependent matrix elements (matrix elements which are not directly computable in the Bethe ansatz). In the single dot case these matrix elements have, at best, only a weak dependence on energy. We would guess that this holds in the double dot case. But we note that regardless of whether the two can be exactly identified (up to a scaling constant), this assumption of equivalence does not affect the exactness of our  $T = 0$  results for transport.

We now turn to what sort of Kondo effect is present at the particle-hole symmetric point. The Kondo singlet that forms at this point involves both electrons sitting on

the two dots. Because we know that an Abrikosov-Suhl resonance forms, we know the electrons are not forming a direct singlet with one another (and indeed, in our model there is no direct interaction between the dots). Rather the singlet formed involving the two localized electrons is mediated by the conduction electrons in the leads. We thus term this Kondo effect an RKKY Kondo effect. We sketch this type of Kondo effect in Figure 5.

It is clear that the RKKY physics occurring here is considerably different than the ferromagnetic interaction that fourth order perturbation theory would predict between closely spaced dots.<sup>40</sup> We see both that RKKY interaction is effectively antiferromagnetic and occurs at an energy scale akin the Kondo temperature. Moreover a strong ferromagnetic interaction would be characterized by a far different conductance. If the two electrons did form an effective spin-1 impurity, the  $T = 0$  conductance would instead be  $2e^2/h$  not the  $0e^2/h$  we universally find.

The ground state associated with the RKKY Kondo effect is Fermi liquid (as will be obvious when we consider

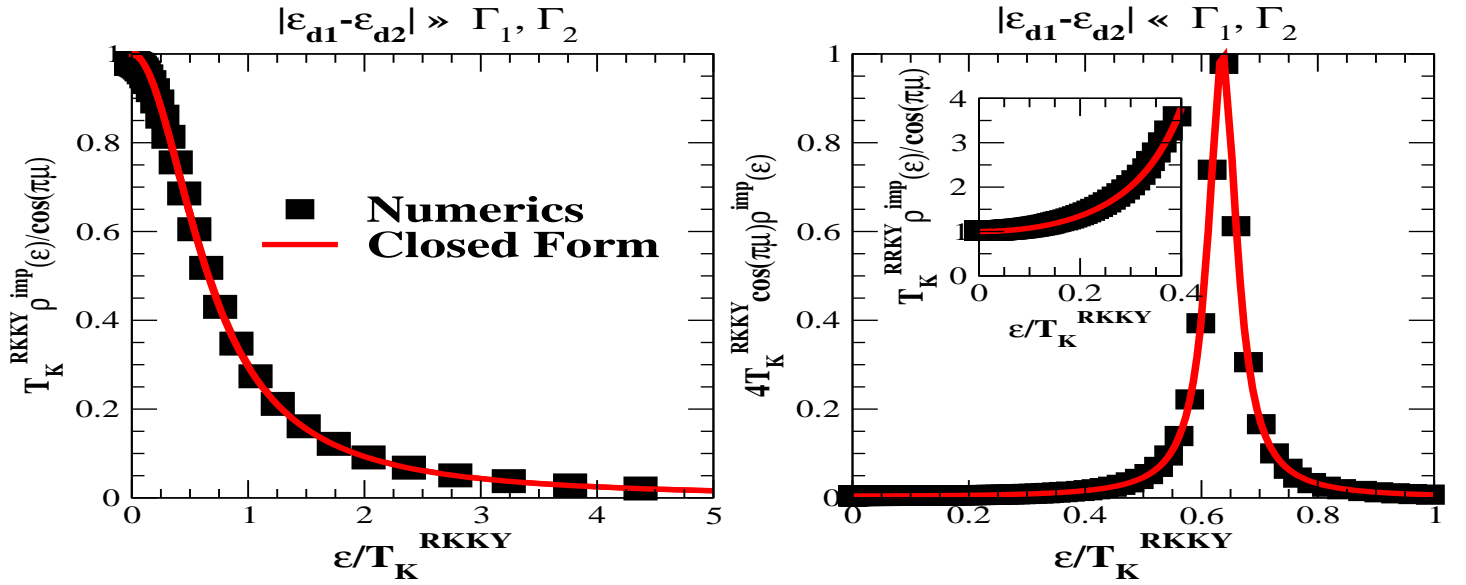


FIG. 4: The low lying impurity density of states (the Abrikosov-Suhl resonance) as a function of energy present in the double dot system at its particle-hole symmetric point. In the left panel we show the shape (Lorentzian) of the resonance for double dots with well separated levels. In the right panel we show the same resonance for the case  $|\epsilon_{d1} - \epsilon_{d2}| \ll \Gamma_{1,2}$  (but  $\epsilon_{d1} \neq \epsilon_{d2}$ ). Here the resonance has split about zero energy by an amount  $4T_K^{\text{RKKY}}/\pi$ .

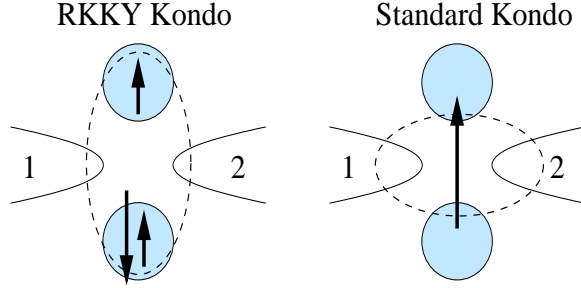


FIG. 5: A cartoon of the two different types of Kondo effects that might appear in the double dot: i) an RKKY Kondo effect where two electrons total sit on the dots and form a singlet mediated through hopping on and off the leads – as this effect depends upon  $\epsilon_{d1} \neq \epsilon_{d2}$ , the dots possess an unequal distribution of electron; and ii) the standard Kondo effect where a single electron sits on the two dots localized primarily in the lower dot level.

the low temperature or low field conductances). This contrasts with the non-Fermi liquid nature of electrons bound into an effective spin-1.<sup>27</sup> It is a check on our results that we do find Fermi liquid physics. We know that the properties of a single dot is perturbative *in the Coulomb repulsion* and so the dot's low temperature fixed point is Fermi liquid. The perturbative structure in the Coulomb repulsion of a double dot is similar in nature. There is then a predilection to believe that the low temperature physics of the double dot should similarly be Fermi liquid. We find further support for our Fermi liquid picture in Ref. 48. While Ref. 48 studied a two impurity Anderson model coupled to two electron chan-

nels (not one as here), they found that the  $T=0$  electron scattering always obeyed the Friedel sum rule, a signature of Fermi liquid physics, no matter the anisotropy between the channels.

Moving away from the particle-hole symmetric point by adjusting  $\epsilon_{d1,2}$  upwards (keeping their relative distance fixed) we uniformly decrease the number of electrons on the dot until we have in total one localized electron. At this point we then expect a standard type Kondo effect to take place. This Kondo effect is akin to that seen in single level dots at their particle-hole symmetric point. While analyzing the Bethe ansatz equations in closed form is difficult, we can nonetheless guess what the associated Kondo temperature is:

$$T_K^{\text{Standard}} = \left( \frac{U_i \Gamma_i}{2} \right)^{1/2} e^{\frac{\epsilon_{d1}(U_1 + \epsilon_{d1})}{2U_1 \Gamma_1}}. \quad (5.5)$$

This formula, available from the analysis of single level dots<sup>35,36,49,50</sup> is valid provided  $|\epsilon_{d1} - \epsilon_{d2}| \ll \Gamma_1, \Gamma_2$  and  $\Gamma_1 \ll U_1$ . In our analysis of the magnetoconductance in the next section we verify that indeed  $T_K^{\text{Standard}}$  as given above governs the physics.

When however  $|\epsilon_{d1} - \epsilon_{d2}| \sim \Gamma_1, \Gamma_2$ , the behaviour of the double dot system with one localized electron appears Kondo like (as determined by the magnetoconductance) over a much narrower range of magnetic field (in units of the Kondo temperature).

As we further increase the gate voltage, we move into a regime characterized by a mixture of interference influenced by strong correlations on the dots. We see non-monotonic behaviour both in the conductance and the number of electrons,  $n_{\text{dis}}$ , displaced by the dots. More-

over if  $|\epsilon_{d1} - \epsilon_{d2}| \gg \Gamma_1, \Gamma_2$  we see that  $n_{\text{dis}}$  can go negative. This requires further explanation.

The Bethe ansatz does not allow one to directly compute the number of electrons,  $n_d$ , occupying the dots. Rather it allows one to compute this number,  $n_d$ , plus  $1/L$  changes of electron occupancy that arise in coupling the leads to the dots. Specifically

$$n_{\sigma\text{dis}} = n_{d\sigma 1} + n_{d\sigma 2} + \int dx \left[ \langle c_{e\sigma}^\dagger(x) c_{e\sigma}(x) \rangle - \rho_{\sigma\text{bulk}} \right] \quad (5.6)$$

where  $\rho_{\sigma\text{bulk}}$  is the density of electrons of spin  $\sigma$  in the leads in the absence of any coupling to the dots. In terms of transport properties, this is a more natural quantity to compute. It is the quantity that is related to the scattering phase by the Friedel sum rule, as the proof of Langreth explicitly shows.<sup>51</sup> We comment on this further in the discussion section.

Now by definition  $n_{d\sigma}$ , the number of electrons on the dots, can never be negative. Thus when we find  $n_{\sigma\text{dis}}$  to be negative, we know that coupling the dots to the leads has induced a *negative*  $1/L$  correction to the lead electron density.

In this non-monotonic regime we see that sharp variations exist in the conductance<sup>20</sup> and are most pronounced if  $|\epsilon_{d1} - \epsilon_{d2}| \gg \Gamma_{1,2}$ . In particular, the variations occur at two values of the gate voltage (i.e.  $\epsilon_{d1}$ ). The first variation is associated with a sudden decrease in the number of localized electrons  $n_{\sigma\text{dis}}$  as  $\epsilon_{d1}$  is lowered while the second variation sees a sudden increase in  $n_{\sigma\text{dis}}$ . We can characterize the two values of  $\epsilon_{d1}$  where these variations occur.

The variations correspond to values of  $\epsilon_{d1}$  where the contribution to the scattering phase from  $K_{i2}$  is rapidly varying (see Eqn. (4.15) of Section IV.A). This rapid variation occurs when  $Q$ , the parameter marking the Fermi surface of the  $\lambda$ -excitations, is close to  $I_i^{-1}$ . Provided  $Q > 0$  we can employ Eqn. (4.16) to parameterize  $Q$  in terms of  $\epsilon_{d1}$ . Equating  $Q$  and  $I_i^{-1}$  then leads to the two values of  $\epsilon_{d1}$  (corresponding to the two values of  $I_{i,2}^{-1}$ ) where the variation occurs

$$\epsilon_{d1} = \left[ \frac{2U_1\Gamma_1}{1 + \frac{1}{2\pi I_i^{-1}}} (I_i^{-1} + \frac{1}{2\pi} - \frac{1}{2\pi} \log(2\pi e I_i^{-1})) \right]^{1/2} - \frac{U_1}{2}. \quad (5.7)$$

The sharpness of these variations in the conductance and  $n_{\sigma\text{dis}}$  are governed by the parameter

$$\gamma_i = \frac{1}{2} |1 - \beta_i^{-1}|,$$

a consequence of  $K_{i2}$  behaving as  $\tan((I_i^{-1} - Q)/\gamma_i)$  for  $I_i^{-1} - Q$  small (see Eqn. (4.15)).  $\gamma_i$  vanishes in the limit  $|\epsilon_{d1} - \epsilon_{d2}| \rightarrow \infty$  while becoming large in the opposite limit. As the two variations in  $n_{\sigma\text{dis}}$  are of the opposite sign, the first of the two variations will induce  $n_{\sigma\text{dis}}$  to go negative if it does not overlap significantly with the

second. Thus the condition for  $n_{\sigma\text{dis}}$  to go negative for some value of the gate voltage is

$$|I_1^{-1} - I_2^{-1}| > \gamma_1 + \gamma_2$$

that is, the spacing of the variations is larger than the sum of their widths. We can translate this into a condition upon the necessary separation of the two levels. We need

$$\begin{aligned} |\epsilon_{d1} - \epsilon_{d2}| &> \frac{b + \sqrt{b^2 + 4ca}}{2a}; \\ a &= \frac{U_1^2 - U_2^2}{4}; \\ b &= \Gamma_1 \Gamma_2 (U_1 + U_2); \\ c &= 2U_i \Gamma_i |\Gamma_2^2 - \Gamma_1^2|, \end{aligned} \quad (5.8)$$

if  $n_{\sigma\text{dis}}$  is to go negative. If  $\Gamma_1, \Gamma_2 \ll U_1, U_2$  this condition simplifies to

$$|\epsilon_{d1} - \epsilon_{d2}| > \left( \frac{8U_i \Gamma_i |\Gamma_2^2 - \Gamma_1^2|}{|U_1^2 - U_2^2|} \right)^{1/2}. \quad (5.9)$$

A note of caution is needed here. This condition is derived under the constraints governing integrability (Eqn. (4.1)). While self-consistent, it should not be used to determine the minimum level separation in two dots with *arbitrary* parameters so as to guarantee  $n_{\sigma\text{dis}}$  will be negative. However one might nonetheless suppose that this condition would provide a rough estimate of the minimum separation for such dots.

Up to this point we have discussed in detail the behaviour of the conductance provided  $\epsilon_{d1}$  is not exactly equal to  $\epsilon_{d2}$ . If instead  $\epsilon_{d1} = \epsilon_{d2}$ , we do not see a marked change in the  $T = 0, H = 0$  linear response conductance. With  $\epsilon_{d1}$  close to  $\epsilon_{d2}$ , we already see in Figure 3d) that the rapid variations in  $G$  associated with interference effects disappear. (This is consistent with the slave boson study of Ref. (19).) And as  $\epsilon_{d1}$  becomes equal to  $\epsilon_{d2}$ , the functional dependence of  $G$  upon the gate voltage remains the same (compare panels c) and d) in Figure 3). However at  $\epsilon_{d1} = \epsilon_{d2}$  there is one significant change. At the particle-hole symmetric point, the RKKY Kondo effect disappears. As this vanishing takes place *discontinuously*,  $\epsilon_{d1} = \epsilon_{d2}$  marks a first order quantum critical point.

This critical behaviour at  $\epsilon_{d1} = \epsilon_{d2}$  has been observed before,<sup>33,52</sup> and can be most easily understood by first appealing to the non-interacting limit. In the non-interacting limit, one can diagonalize the dot degrees of freedom via the transformation,

$$d_{\text{even/odd}} = \frac{1}{\sqrt{\Gamma_1^2 + \Gamma_2^2}} (\Gamma_{1/2} d_1 \pm \Gamma_{2/1} d_2),$$

and so we have a system where only one dot level is tied to the leads.<sup>53</sup> This mapping is tied to a dramatic change in

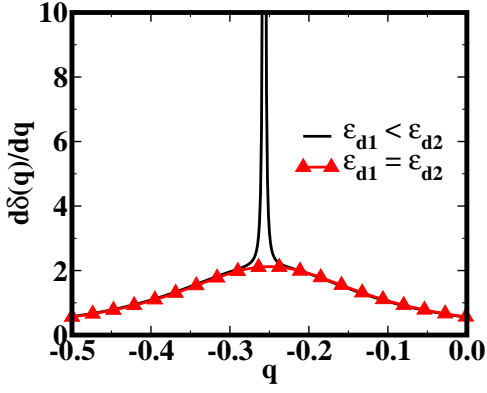


FIG. 6: The impurity density of states for a non-interacting double dot system when  $\epsilon_{d1}$  and  $\epsilon_{d2}$  are close but not exactly equal and for when  $\epsilon_{d1} = \epsilon_{d2}$ . We see that at  $\epsilon_{d1} \rightarrow \epsilon_{d2}$ , there is a discontinuous change in the density of states.

the non-interacting density of states (see Figure 6). We see that with  $\epsilon_1$  and  $\epsilon_2$  nearly equal but still different, the impurity density of states possesses a sharply peaked feature not present when  $\epsilon_1 = \epsilon_2$ . It is this feature that permits the formation of the Abrikosov-Suhl resonance when interactions are turned on. Its absence at  $\epsilon_1 = \epsilon_2$  explains the absence of the RKKY Kondo effect. While interactions will couple the second (odd) dot level to the system, the absence of direct hopping to the odd level means that the RKKY Kondo effect cannot develop. Instead, the two electrons bind directly into a singlet and the Kondo effect is entirely absent.

We point out that the particular behaviour observed at  $\epsilon_{d1} = \epsilon_{d2}$  is dependent on there being no coupling between the two dots (whether it be tunnel or capacitive coupling). If the dots are coupled, the two levels will be split by the coupling (for example, a tunneling term will lead to split bonding/antibonding dot levels).<sup>17,18</sup>

### B. Finite Field Linear Response Conductance at the Dots' Particle-Hole Symmetric Point

We now consider the conductance of the double dots at the particle-hole symmetric point. As we have discussed in the previous section, this point sees the formation of an RKKY Kondo effect with an attendant Abrikosov-Suhl

resonance. The presence of this resonance governs intimately how the conductance evolves as Zeeman fields on the order of the RKKY Kondo temperature are applied to the dots as it represents the sole available low energy degrees of freedom.

The shape of the Abrikosov-Suhl resonance thus determines the form of the magnetoconductance as a function of magnetic field. In the case that  $|\epsilon_{d1} - \epsilon_{d2}| \gg \Gamma_{1,2}$ , the Abrikosov-Suhl resonance has a Lorentzian form (see the right panel of Figure 4) with a peak centered at zero energy. As a Zeeman field is turned on, the magnetoconductance will thus immediately depart from its particle-hole symmetric value ( $0e^2/h$ ). The universal form of the  $G(H)$  in this case is shown in the rightmost panel of Figure 7. We plot both the closed form available from the analysis performed in Section IV.B as well as a direct numerical evaluation of the Bethe ansatz integral equations. We see we obtain an excellent match (thus validating the approximations used in solved these equations analytically). We see that the magnetoconductance peaks at the maximal possible conductance for a value of  $H$  corresponding to  $1.4T_K^{\text{RKKY}}$ . That it does reach the unitary maximum is a reflection of the fact that the scattering phases for spin up and down electrons are symmetric about  $2\pi$  (see Eqn. (4.24)). After reaching the unitary maximum the magnetoconductance decreases uniformly behaving as  $1/\log^2(H/T_K^{\text{RKKY}})$  for  $H \gg T_K^{\text{RKKY}}$ .

In the second panel of Figure 7 we plot the magnetoconductance for the case  $|\epsilon_{d1} - \epsilon_{d2}| \ll \Gamma_{1,2}$ . The functional form of the magnetoconductance in this case is also governed by the shape of the Abrikosov-Suhl resonance. As shown in the left panel of Figure 4, the resonance here is peaked at an energy  $\epsilon = T_K^{\text{RKKY}}$ . While it does not vanish at zero energy, its value relative to its peak value is  $4\cos^2(\pi\mu)$  where  $\mu$  is defined in Eqn. (5.2) and here is approximately 1/2. Consequently the change in the conductance in this case upon the initial introduction of a magnetic field will be negligible. But once the magnetic field reaches a strength of  $T_K^{\text{RKKY}}$ , the magnetoconductance will undergo an extremely rapid variation (as seen in Figure 7). Once the unitary maximum is reached, the magnetoconductance again decreases monotonically behaving as  $1/\log^2(H/\tilde{T}_K^{\text{RKKY}})$ .

We can summarize the behaviour of the magnetoconductance in these two cases via

$$G = \begin{cases} \frac{2e^2}{h} \frac{\pi^2}{4} \cos^2(\pi\mu) \left( \frac{H}{T_K^{\text{RKKY}}} \right)^2 + \mathcal{O}\left( \frac{H}{T_K^{\text{RKKY}}} \right)^4; & \text{if } H \ll T_K^{\text{RKKY}}, \\ \frac{\pi^2}{2\log^2(H/\tilde{T}_K^{\text{RKKY}})} - \frac{\pi^4\mu^2}{\log^4(H/\tilde{T}_K^{\text{RKKY}})} + \mathcal{O}\left( \frac{\log \log(H/\tilde{T}_K^{\text{RKKY}})}{\log^3(H/\tilde{T}_K^{\text{RKKY}})} \right) + \mathcal{O}\left( \frac{\mu^2 \log \log(H/\tilde{T}_K^{\text{RKKY}})}{\log^5(H/\tilde{T}_K^{\text{RKKY}})} \right) + \mathcal{O}\left( \frac{\mu^4}{\log^6(H/\tilde{T}_K^{\text{RKKY}})} \right), & \text{if } H \gg T_K^{\text{RKKY}}, \end{cases} \quad (5.10)$$

where  $\tilde{T}_K^{\text{RKKY}} = \frac{2^{3/2}}{\sqrt{\pi e}} T_K^{\text{RKKY}}$ . In the above expression

for the conductance in the limit  $H \gg \tilde{T}_K^{\text{RKKY}}$  we have

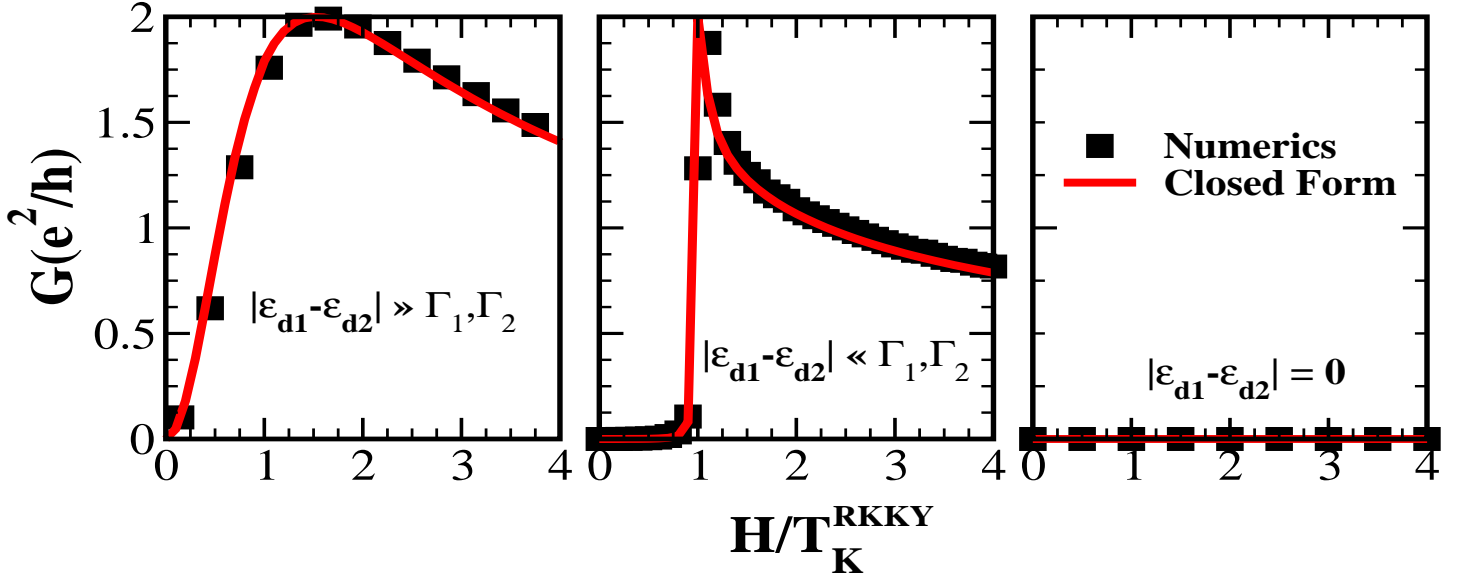


FIG. 7: Plotted is the magnetoconductance of the double dot system at its particle-hole symmetric point. We consider three cases: right panel ( $|\epsilon_{d1} - \epsilon_{d2}| \gg \Gamma_{1,2}$ ), middle panel ( $|\epsilon_{d1} - \epsilon_{d2}| \ll \Gamma_{1,2}$ ), and left panel ( $|\epsilon_{d1} - \epsilon_{d2}| = 0$ ).

included the leading order term in  $\mu^2$  as this governs the different behaviour in the two cases  $|\epsilon_{d1} - \epsilon_{d2}| \ll \Gamma_{1,2}$  and  $|\epsilon_{d1} - \epsilon_{d2}| \gg \Gamma_{1,2}$ .

We now consider the final case when  $\epsilon_{d1} = \epsilon_{d2}$ . As discussed previously, in this instance, the Abrikosov-Suhl resonance identically vanishes. Without the Abrikosov-Suhl resonance and the concomitant absence of a low energy density of states, the conductance is unchanged upon application of a Zeeman field on the order of  $T_K^{\text{RKKY}}$  (see righthand panel of Figure 7). (We note that when  $\epsilon_{d1} = \epsilon_{d2}$  there is no Kondo temperature. The plot in the righthand panel of Figure 7 is made taking the Kondo temperature as defined in the case  $|\epsilon_{d1} - \epsilon_{d2}| \sim 0$  but not exactly 0.)

### C. Finite Field Linear Response Conductance as a Function of Gate Voltage

We now consider the magnetoconductance away from the particle-hole symmetric point. As with this point, the changes induced in the conductance by the application of a magnetic field is determined by the presence or absence of an Abrikosov-Suhl resonance. If a resonance is present, we in general marked changes by the introduction of even a small Zeeman field. If however the resonance is absent (solely in the case  $|\epsilon_{d1} - \epsilon_{d2}| = 0$ ), the conductance will only be sensitive to Zeeman fields on the order of the

bare parameters in the model.

In the top panel of Figure 8 we first consider the case of  $|\epsilon_{d1} - \epsilon_{d2}| \gg \Gamma_{1,2}$ , plotting  $G$  as a function of gate voltage (i.e.  $\epsilon_{d1}$ ) for a variety of values of Zeeman field ranging from  $H = \Gamma_1/500$  to  $H = 3\Gamma_1$ . As expected from the previous section even the smallest of these field strengths strongly alters the conductance near the particle hole symmetric point (we note that  $T_K^{\text{RKKY}} = 0.00243\Gamma_1$ ). The region of  $\epsilon_{d1}$  over which the conductance is altered from its zero field value significantly increases as  $H$  is increased. As  $\epsilon_{d1}$  is initially decreased, we see that the conductance tracks closely its zero field value (as displayed in the top left panel of Figure 3). However a value of  $\epsilon_{d1}$  is inevitably reached where the conductance markedly changes. For the smallest field value used,  $H = \Gamma_1/500$ , this occurs at  $\epsilon_{d1} \approx -6\Gamma_1$  while for largest,  $H = 3\Gamma_1$ , large scale deviations in  $G$  begin at  $\epsilon_{d1} \approx \Gamma_1$ .

For the smaller values of the field used, the conductance sees a local maximum around  $\epsilon_{d1} = -6\Gamma_1$ . This is the position of the (standard) Kondo effect we argued to exist at zero field in the first part of this section. The Kondo temperature for this effect is  $T_K^{\text{Standard}} = 0.00422\Gamma_1$ , twice the smallest value of field ( $H = .002\Gamma_1$ ) displayed in Figure 8. As the magnetic field is increased, the conductance in the vicinity of  $\epsilon_{d1}$  decreases as would be expected for the standard Kondo effect.

We plot this decrease in the conductance maximum as a function of  $H$  in Figure 9. From Ref. (36), the expected

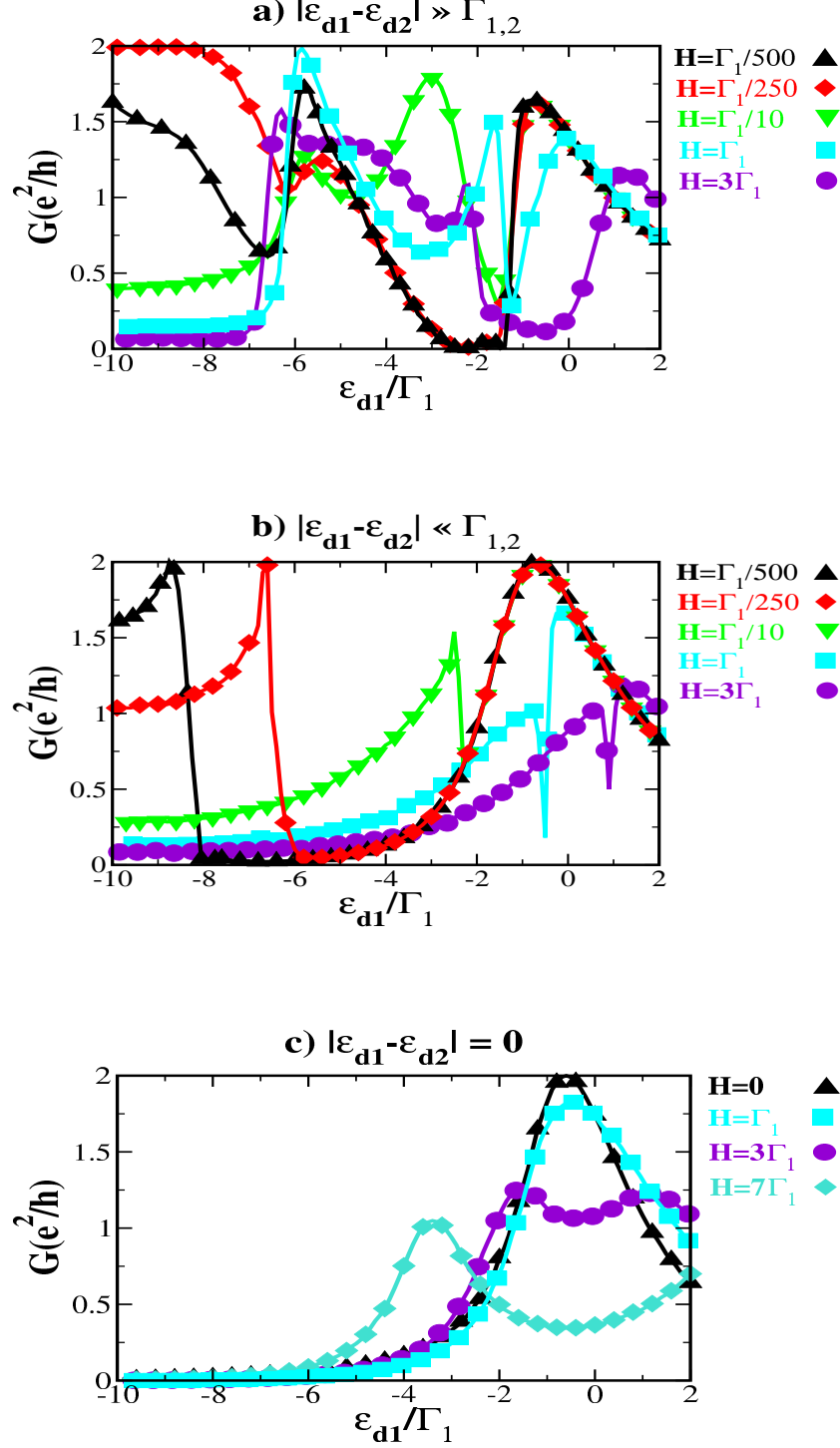


FIG. 8: Plots of the conductance as a function of  $\epsilon_{d1}$  for a variety of values of Zeeman field,  $H$ . We consider three cases: a)  $|\epsilon_{d1} - \epsilon_{d2}| \gg \Gamma_{1,2}$ ; b)  $|\epsilon_{d1} - \epsilon_{d2}| \ll \Gamma_{1,2}$ ; c)  $|\epsilon_{d1} - \epsilon_{d2}| = 0$ . In all three  $U_1 = 1$  and  $\Gamma_1 = U/20$ . For a) and b) we see sharp changes in  $G$  closely tied to the presence of an Abrikosov-Suhl resonance at  $H = 0$ . For c) the resonance is absent and changes in  $G$  occur only when  $H$  exceeds  $\Gamma_1$ .

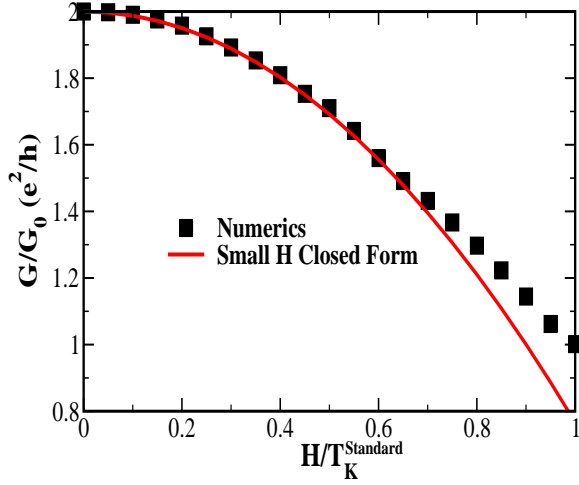


FIG. 9: A plot of the magnetoconductance for the case  $|\epsilon_{d1} - \epsilon_{d2}| \gg \Gamma_{1,2}$  at a value of the gate voltage where one localized electron is found on the dots. We use the same parameters as in Figure 8. We plot both the results of a numerical analysis of the Bethe ansatz equations as well as the small field analytic form that would be expected if the system was a single dot.

from of this decrease is

$$G(H) = G(H=0) \left(1 - \frac{\pi^2}{16} \left(\frac{H}{T_K^{\text{Standard}}}\right)^2\right). \quad (5.11)$$

We see in Figure 9 that the numerical analysis of the Bethe ansatz equations follows this form for values of the Zeeman field up to  $T_K^{\text{Standard}}$ .

The plot in Figure 9 was produced in the case  $|\epsilon_{d1} - \epsilon_{d2}| \gg \Gamma_{1,2}$ . As this condition is relaxed, the standard Kondo effect does not disappear. However the region of field over which Eqn. (5.11) is valid decreases.

In the middle panel of Figure 8 we consider the magnetoconductance in the case  $|\epsilon_{d1} - \epsilon_{d2}| \ll \Gamma_{1,2}$ . In this case the conductance behaves in much the same fashion as  $|\epsilon_{d1} - \epsilon_{d2}| \gg \Gamma_{1,2}$ . For the smallest values of the field the conductance goes unaltered from its zero field value over a substantial range of gate voltages. This range shrinks as  $H$  increases. And when the conductance ceases to track its  $H=0$  value, it does so abruptly. Due to the nature of the Abrikosov-Suhl in this case (i.e. a resonance sharply peaked about  $\epsilon = T_K^{\text{RKKY}}$ ), we find that the changes in the linear response conductance, when they occur, to be even more marked. Even for fields for in excess of  $T_K^{\text{RKKY}}$  (in this case  $T_K^{\text{RKKY}} = 0.00179\Gamma_1$ ), we see sharp changes persist in the magnetoconductance. For both  $H = \Gamma_1$  and  $H = 3\Gamma_1$  we see that there are sharp downward changes in the conductance for values of  $\epsilon_{d1}$  near 0.

In the final panel of Figure 8 we plot the magnetoconductance in the case  $|\epsilon_{d1} - \epsilon_{d2}| = 0$ . Here there is no Abrikosov-Suhl resonance at the particle-hole symmetric point. With the absence of a dynamically enhanced low energy density of states, we find  $G$  to be insensitive to values of  $H$  smaller than the bare parameters. The conductance is approximately equal to its zero field value

until  $H$  becomes of the same magnitude as  $\Gamma_1$ . For values of  $H$  in excess of  $\Gamma_1$  we see that the zero field peak at  $\epsilon_{d1} \sim -\Gamma_1$  splits in two with increasing separation as  $H$  grows.

## VI. FINITE TEMPERATURE TRANSPORT OF DOUBLE DOT

In this section we analyze the finite temperature linear response conductance,  $G(T)$ , at the particle-hole symmetric point. As with the magnetoconductance at this point, the behaviour of  $G(T)$  at temperatures on the order of  $T_K^{\text{RKKY}}$  is ultimately determined by the form of the low energy density of states, that is, the Abrikosov-Suhl resonance as given in Eqn. (5.4). In particular, the nature of the Abrikosov-Suhl resonance marks the difference between the two opposing limits of the bare level separation, i.e.  $|\epsilon_{d1} - \epsilon_{d2}| \gg \Gamma_{1,2}$  and  $|\epsilon_{d1} - \epsilon_{d2}| \ll \Gamma_{1,2}$ .

To evaluate the finite temperature conductance, we solve numerically through iteration the equations in (3.22) and (3.26). To do so we approximate the source term for the integral equation governing  $\rho^{\text{imp}}(k)$  by Eqn. (5.1), an excellent approximation provided we are at the particle-hole symmetric point. Then following the procedure described in Section III.C, we obtain the results plotted in Figure 9.

In the case  $|\epsilon_{d1} - \epsilon_{d2}| \gg \Gamma_{1,2}$  (see the left panel of Figure 9), the Abrikosov-Suhl resonance is peaked at zero energy. Thus even for temperatures far below the Kondo temperature,  $T_K^{\text{RKKY}}$ , we see an immediate change in the conductance from its zero temperature value ( $0e^2/h$ ). For temperatures far below  $T_K^{\text{RKKY}}$  the conductance has a quadratic Fermi liquid form which we can determine to be

$$G(T) = \frac{2e^2}{h} \frac{\pi^4 \cos^2(\mu\pi)}{4} \left(\frac{T}{T_K^{\text{RKKY}}}\right)^2. \quad (6.1)$$

We can determine this form by comparing the analysis of the Bethe ansatz equations at finite temperature for a single level dot.<sup>36</sup> For a single level dot (sld) the Abrikosov-Suhl resonance is given by

$$\rho^{\text{imp sld}}(\epsilon, T_K^{\text{sld}}) = \frac{1}{2T_K^{\text{sld}}} \frac{1}{1 + \frac{\pi^2 \epsilon^2}{4(T_K^{\text{sld}})^2}}. \quad (6.2)$$

For a double dot (dd) with well-separated bare levels (i.e.  $\mu \sim 0$ ), the Abrikosov-Suhl resonance has the same form (see Eqn. (5.4))

$$\rho^{\text{imp dd}}(\epsilon, T_K^{\text{RKKY}}) = 2 \cos(\mu\pi) \rho^{\text{imp sld}}(\epsilon, T_K^{\text{RKKY}}). \quad (6.3)$$

This in turn implies that an electron with energy  $\epsilon$  scatters off the double dot via the relation

$$\delta_{\text{el}}^{\text{dd}}(T, \epsilon) = 2 \cos(\mu\pi) \delta_{\text{el}}^{\text{sld}}(T, \epsilon). \quad (6.4)$$

This relation follows because the Abrikosov-Suhl resonance serves as the source term governing the *linear* integral equations determining the scattering phase. For a

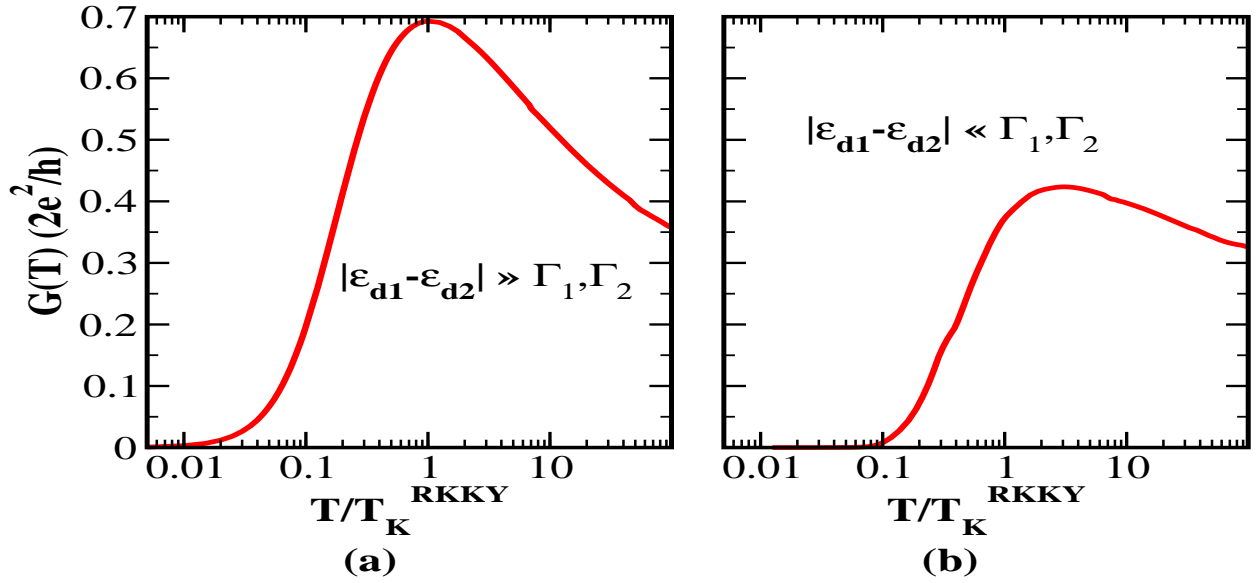


FIG. 10: Plots of the finite temperature linear response conductance in the cases  $|\epsilon_{d1} - \epsilon_{d2}| \gg \Gamma_{1,2}$  (left panel (a)) and  $|\epsilon_{d1} - \epsilon_{d2}| \ll \Gamma_{1,2}$ . In both cases we employ  $U_1 = 1$  and  $\Gamma_1 = U/20$ . For (a) we use a bare level separation of  $\epsilon_{d2} - \epsilon_{d1} = 5\Gamma_1$  while for (b)  $\epsilon_{d2} - \epsilon_{d1} = 0.5\Gamma_1$ .

single level dot, the deviation of the finite temperature linear response conductance from its zero temperature value takes the form,<sup>36,50</sup>

$$\delta G(T) = \frac{2e^2}{h} \frac{\pi^4}{16} \frac{T^2}{(T_K^{\text{sl}})^2}.$$

As  $G(T) = \int \partial_E f(E) \sin^2(\delta_{\text{el}}(E, T))$ , we see that for  $\delta_{\text{el}}(E)$  small, the low temperature form of  $G(T)$  for the single level dot determines  $G(T)$  for the double dot to be given as in Eqn. (6.1).

As the temperature is increased,  $G(T)$  reaches a maximum at roughly  $T = T_K^{\text{RKKY}}$ . With further increases,  $G(T)$  decreases from its maximal value (for the parameters chosen,  $1.4e^2/h$ ) gradually. For large values of temperature we see that the conductance decreases logarithmically. From the behaviour of  $G(T \gg T_K)$  for a single level dot (Ref. (54)) and the similarity of analysis between that case and a double dot, we might expect

$$G(T \gg T_K^{\text{RKKY}}) \sim \frac{1}{\log^2(T/T_K^{\text{RKKY}})}. \quad (6.5)$$

However from examining panel (a) of Figure 9, it is clear that if this behaviour does hold, it is valid only for temperatures much larger than  $10T_K^{\text{RKKY}}$  (in the range  $10T_K^{\text{RKKY}} - 100T_K^{\text{RKKY}}$ , Figure 9 implies the conductance is decreasing at best according to  $1/\log(T/T_K^{\text{RKKY}})$ ). This however is unsurprising as a similar condition holds on the finite temperature behaviour of a single level dot for  $T \gg T_K$ .

In panel (b) of Figure 9 we plot  $G(T)$  for the case of  $|\epsilon_{d1} - \epsilon_{d2}| \ll \Gamma_{1,2}$ . In this case the Abrikosov-Suhl resonance has a sharp peak at an energy  $\epsilon = T_K^{\text{RKKY}}$  with

minimal (although finite) spectral weight at zero energy. We thus expect that the low temperature response to be much smaller than for the case  $|\epsilon_{d1} - \epsilon_{d2}| \gg \Gamma_{1,2}$ . And we see this in Figure 9 where  $G(T)$  is effectively  $0e^2/h$  (equal to its zero temperature value) until  $T \sim 0.1T_K^{\text{RKKY}}$ . For  $T \ll T_K^{\text{RKKY}}$ ,  $G(T)$  has the exact same form as given in Eqn. (6.1) for the case  $|\epsilon_{d1} - \epsilon_{d2}| \gg \Gamma_{1,2}$ . However here  $\mu \sim 1/2$  and so the coefficient of the  $T^2$  correction is extremely small.

As the temperature is increased in this case to roughly  $2T_K^{\text{RKKY}}$ , a maximum occurs in the conductance (for the particular parameters chosen). While the value at which the maximum occurs is non-universal, we do expect it to roughly occur when the temperature is  $\mathcal{O}(T_K^{\text{RKKY}})$ . With further increases in temperature, the conductance logarithmically decreases. If this decrease is to behave as  $G \sim 1/\log^2(T/T_K^{\text{RKKY}})$  (as for a single level dot), the temperature at which this asymptotic form begins to be valid is far in excess of  $10T_K^{\text{RKKY}}$ .

## VII. DISCUSSION

### A. Friedel Sum Rule

The Friedel sum rule relates the scattering phase,  $\delta_{\sigma e}$ , of an electron of spin  $\sigma$  at the Fermi surface at zero temperature to the number of electrons displaced by connecting the leads to the dot,  $n_{\sigma \text{dis}}$ :

$$\delta_{\sigma e} = 2\pi n_{\sigma \text{dis}}. \quad (7.1)$$

$n_{\sigma\text{dis}}$  has two contributions: 1) the number of localized electrons sitting on the dot and equal to,

$$\sum_{\alpha} \langle d_{\sigma\alpha}^{\dagger} d_{\sigma\alpha} \rangle$$

and 2) the  $1/L$  deviations induced in the electron number in the leads

$$\delta n_{\text{leads}} = \int dx \left[ \langle c_{\sigma e}^{\dagger}(x) c_{\sigma e}(x) - \rho_{\sigma\text{bulk}} \right],$$

where  $\rho_{\sigma\text{bulk}} = L/2\pi$  is the bulk interacting density of states of the leads with the leads and dots unconnected to one another. While this second contribution is typically not considered in the application of the Friedel sum rule, its proof explicitly takes it into account.<sup>51</sup>

We have already seen that in the model of double dots analyzed here that this second contribution,  $\delta n_{\text{leads}}$ , is non-negligible and in fact can be negative, driving  $n_{\sigma\text{dis}}$  itself negative (and thus cannot be ignored if the conductance is to be computed correctly). The range of gate voltages where this occurs marks a region of rapid variation in the conductance (see the top left panel of Figure 3 for example). The possibility that this second contribution is non-zero is closely tied to the presence of two interfering pathways for the electrons to transit the dot system. A finite value for  $\delta n_{\text{leads}}$  has also been seen in the analysis of Fano resonances in quantum dots.<sup>41</sup> For dots exhibiting Fano resonances, there are two tunneling paths between the leads: one resonant inducing a single particle scattering phase,  $\delta(q) = -2 \tan^{-1}(\Gamma/(q - \epsilon_d))$  and a non-resonant second path with a constant scattering phase. The two paths, however, interfere and the overall scattering phase is more complicated than the mere sum of the two (akin to the fact the sum of the bare scattering phase off the double dots in Eqn. (2.4) has the sum in the argument of  $\tan^{-1}$ ). The system exhibiting Fano resonances may be considered a certain limit of the double dots studied here. If we take the limit of  $\epsilon_{d2}$  and  $\Gamma_2$  in such a way that

$$\frac{\Gamma_2}{q - \epsilon_{d2}}$$

is constant for all wavevectors  $q$  we recover the physics of Fano resonances.

$n_{\sigma\text{dis}}$  is a quantity naturally available from the Bethe ansatz as the Bethe ansatz allows one to directly access the scattering phase, i.e. the formalism, as discussed in Section III, provides a means to derive the scattering phase independent of directly invoking the Friedel sum rule. In this sense we provide a proof of the Friedel sum rule in the case of a double dot system. We do note that however we are able to compute in principle the occupation of the dots  $\sum_{\alpha} \langle d_{\sigma\alpha}^{\dagger} d_{\sigma\alpha} \rangle$  by computing the impurity free energy and then taking appropriate derivatives with respect to  $\epsilon_{d\alpha}$ .

## B. The Effects of Breaking Integrability

We now turn to the question of how finely tuned the results presented herein are. Our ability to exactly solve the models of the double dots depends upon the constraints listed in Eqn. (2.8) being satisfied. However it is important to determine how the physics is affected if these conditions are broken, at least weakly. While it is easily conceivable that an experimental double dot system could be tuned so that its parameters satisfy approximately the constraints of Eqn. (2.8), we cannot hope that the constraints are met *exactly*.

Fortuitously, we do not expect any of the major phenomena identified in this paper to change qualitatively if Eqn. (2.8) is weakly violated. Generally, we expect the physics to be perturbative in any deviation from the conditions necessary for integrability. To see this, contrast the situation of a single dot coupled to a single lead. This problem is non-perturbative in the dot-lead coupling, a partial consequence of the ambiguous nature of the zeroth order zero temperature dot density matrix about which one conducts the perturbation theory. This is true both in the presence and absence of interactions. Indeed it is relatively straightforward to derive the dots' Green functions at  $U = 0$  and see that they do not have a well-defined  $V \rightarrow 0$  limit. Concomitantly, perturbation theory in  $U$ , the dot Coulomb repulsion, is well behaved as the dot Green's function is unambiguously defined at  $U = 0$  by the presence of the dot-lead hybridization. Similarly if we weakly break one of the integrability constraints, we expect the deviation to behave in a perturbative fashion as the dot state is already robustly established. This principle guided the study of perturbations about the exactly solvable Toulouse limit of a non-equilibrium dot in Ref. (55).

Now while small deviations from the integrability constraints will only quantitatively change the physics, the same cannot be said of large deviations. In Ref. (28) a particle-hole symmetric double dot is considered where  $\epsilon_{d1} = -U_1/2$ ,  $\epsilon_{d2} = U_2 = 0$ , and  $V_1, V_2$  finite. These conditions represent a strong violation of the integrability condition,  $V_2^2 U_2 = V_1^2 U_1$ . And instead of a Kondo effect, the double dot is found to be in a local moment regime.

There are other more specific arguments as to why violating the integrability constraints will not drastically change the physics. To this end, let us consider the constraint upon the left-right hopping amplitudes. If this constraint is met, only one electron channel couples to the dot (the even channel), while the second channel is decoupled. Let us consider the effects of weakly violating this condition. The second (odd) channel then couples to the dots. However this will change qualitatively none of the Kondo physics discussed in the manuscript. In principle, the second channel *could* introduce a second Kondo scale,  $T_{K2}$  (for either the RKKY Kondo effect or the regular Kondo effect) as in Ref. (56). If we start at some high temperature and begin to lower it, when  $T$  reaches  $T_{K1}$  (the Kondo temperature associated with the even

channel and given in the manuscript) the Kondo singlets (either RKKY or standard) will establish themselves. If we continue to lower the temperature to  $T_{K2}$  nothing further will happen as there are no spin degrees of freedom (the state is a singlet) left to screen. (This contrasts with Ref. (56) where an effective spin- $S$  ( $S \geq 1$ ) impurity was envisioned and a two-stage Kondo effect was predicted to occur).

Another argument that demonstrates the RKKY Kondo effect is not a result of fine tuning makes appeal to a Schrieffer-Wolfe transformation at the particle-hole symmetric point. Under such a transformation the Hamiltonian reduces to the form,

$$H = H_{\text{conduction electrons}} + J_1 S_1 \psi^\dagger \sigma \psi + J_2 S_2 \psi^\dagger \sigma \psi, \quad (7.2)$$

where the two couplings,  $J_i$ , are given by

$$J_i = \frac{2\Gamma_i}{U + \epsilon_{di}} - \frac{2\Gamma_i}{\epsilon_{di}}.$$

We see that generically  $J_1 \neq J_2$  for the integrable range of parameters and that deviations away from the integrability constraints do not change this fact. Thus we would expect such deviations to affect only non-universal aspects of the physics (such as the exact values of Kondo temperatures).

While a small breaking of the integrability conditions will not destroy the RKKY Kondo effect, there is one small perturbation that will. The RKKY Kondo effect involves singlet formation of two electrons sitting on two dots as mediated by the electrons sitting in the leads. But if one were to add a coupling,  $J_{\text{singlet}}$ , in excess of the Kondo temperature,  $T_K^{\text{RKKY}}$ , that promoted direct singlet formation between the two localized electrons, i.e.  $\delta H = J_{\text{singlet}} S_1 \cdot S_2$ , we would expect to destroy the RKKY Kondo effect. In principle, any experimental realization of a double dot system will contain such a  $J_{\text{singlet}}$ . And because  $T_K^{\text{RKKY}}$  is exponentially small compared to the bare parameters, one might think that the RKKY Kondo effect will be generically overcome. While this may be true at the particle-hole symmetric point, the RKKY Kondo effect exists over a range of gate voltages centered around this point. By tuning the gate voltage to different values within this range, one can increase  $T_K^{\text{RKKY}}$  above any putative value of  $J_{\text{singlet}}$ .

We finally turn to the effects of breaking the integrability conditions on the the quantum critical point at  $\epsilon_{d1} = \epsilon_{d2}$ . We note that this point is tied to the disappearance of a singular feature in the non-interacting impurity density of states at  $\epsilon_{d1} = \epsilon_{d2}$  (see Figure 6). In turn this disappearance is dependent upon the decoupling of the odd dot degree of freedom,  $d_{\text{odd}}$ . A perturbation that restores this coupling (such as weakly coupling a second channel of electrons to the dots) will change the critical point to a smooth crossover and so restore the RKKY Kondo effect, but a perturbation which leaves  $d_{\text{odd}}$  uncoupled (such as perturbations on the inter-/intra-dot Coulomb repulsion) will presumably leave the critical point in place.

## Acknowledgments

This work was supported by the DOE under contract DE-AC02-98 CH 10886.

## APPENDIX A: WIENER-HOPF ANALYSIS OF EQUATIONS GOVERNING THE LINEAR RESPONSE CONDUCTANCE

### 1. Review of Wiener-Hopf Analysis

We review the method of solution as presented in Ref. (35) for equations of the general form

$$f(z) = \int_{-\infty}^A dz' f(z') h(z - z') + g(z). \quad (A1)$$

Writing  $f^\pm(z) = f(z)\theta(\pm z \mp A)$ , the Fourier transform of the above equation yields

$$f^+(\omega) + f^-(\omega) = f^-(\omega)h(\omega) + g(\omega), \quad (A2)$$

where Fourier transforms are defined by

$$a(\omega) = \int d\omega e^{i\omega z} a(z). \quad (A3)$$

The key step in the analysis is writing  $1 - h(\omega)$  as a product of functions,  $G^\pm$ , which are analytic in the upper/lower planes respectively:

$$1 - h(\omega) = \frac{1}{G^+(\omega)G^-(\omega)}. \quad (A4)$$

We can then write Eqn.(A2) as

$$e^{-i\omega A} \frac{f^-(\omega)}{G^-(\omega)} + e^{-i\omega A} f^+(\omega) G^+(\omega) = g(\omega) G^+(\omega) e^{-i\omega A}. \quad (A5)$$

Given  $e^{-i\omega A} f^\pm(\omega)$  is analytic in the upper/lower half plane, applying the operators

$$\pm \frac{1}{2\pi i} \int d\omega' \frac{1}{\omega' - (\omega \pm i\delta)}, \quad (A6)$$

to Eqn.(A5) yields solutions for both  $f^+$  and  $f^-$ :

$$\begin{aligned} f^-(\omega) &= -G^-(\omega) \frac{e^{i\omega A}}{2\pi i} \\ &\times \int d\omega' \frac{1}{\omega' - (\omega - i\delta)} g(\omega') G^+(\omega') e^{-i\omega' A}; \\ f^+(\omega) &= \frac{e^{i\omega A}}{G^+(\omega)} \frac{1}{2\pi i} \\ &\times \int d\omega' \frac{1}{\omega' - (\omega + i\delta)} g(\omega') G^+(\omega') e^{-i\omega' A}. \end{aligned} \quad (A7)$$

## 2. A Wiener-Hopf Analysis of the Scattering Phase Analysis of Zero Field

The scattering phase can be written as

$$\begin{aligned}\delta_e &= 2\pi \int_Q^\infty d\lambda(\sigma_1(\lambda) + \sigma_2(\lambda)); \\ &= 2\pi - \pi \int_{-\infty}^Q d\lambda(\sigma_1(\lambda) + \sigma_2(\lambda)).\end{aligned}\quad (\text{A8})$$

where each  $\sigma_i(\lambda)$  satisfies

$$\begin{aligned}\sigma_i^{\text{imp}}(\lambda) &= \int_{-\infty}^Q d\lambda' R(\lambda - \lambda') \sigma_i^{\text{imp}}(\lambda') \\ &+ \text{sgn}(1 - \beta_i) \int_{-\infty}^\infty d\lambda' (1 + a_2)^{-1} (\lambda - \lambda') a_{|1 - \beta_i^{-1}|}(\lambda') \\ &+ \int_{-\infty}^\infty dq s(\lambda - g(q)) \Delta_{0i}(q).\end{aligned}\quad (\text{A9})$$

The above two equations can be obtained by inverting via Fourier transform Eqn.(4.8).

Identifying

$$\begin{aligned}g(\omega) &= \frac{1}{1 + e^{-|\omega|}} \left( e^{-|\omega|/2} \int_{-\infty}^\infty dq \Delta_{0i}(q) e^{i\omega g(q)} \right. \\ &\quad \left. + \text{sign}(1 - \beta_i) \frac{e^{-\gamma_i|\omega| + i\omega I_i^{-1}}}{1 + e^{-|\omega|}} \right); \\ \gamma_i &= -\frac{1}{2}(1 - \beta_i^{-1})\text{sign}(1 - \beta_i); \\ I_i^{-1} &= \frac{\alpha_i^2 - \tilde{\Gamma}_i^2}{2U_i\Gamma_i}; \\ G^\pm(\omega) &= \frac{\sqrt{2\pi}}{\Gamma(1/2 \mp i\omega/2\pi)} \left( \frac{\mp i\omega + \delta}{2\pi e} \right)^{\mp i\omega/2\pi},\end{aligned}\quad (\text{A10})$$

where  $\beta_i$  and  $\alpha_i$  are defined in Eqns.(4.5), we apply the Wiener-Hopf methodology presented at the beginning of this section to compute

$$\int_{-\infty}^Q d\lambda \sigma_i(\lambda) = \sigma_i^-(\omega = 0). \quad (\text{A11})$$

We so find

$$\int_{-\infty}^Q d\lambda \sigma_i(\lambda) = K_{i1} + K_{i2}; \quad (\text{A12})$$

where

$$\begin{aligned}K_{i1} &= -\frac{1}{2\pi^{3/2}i} \int d\omega \frac{1}{\omega + i\delta} \left( \frac{-i\omega + \epsilon}{2\pi e} \right)^{-\frac{i\omega}{2\pi}} \\ &\times \Gamma\left(\frac{1}{2} + \frac{i\omega}{2\pi}\right) \int_{-\infty}^\infty dq \Delta_{0i}(q) e^{i\omega(g(q) - Q)} \\ K_{i2} &= \text{sign}(\beta_i - 1) \frac{1}{2\pi^{3/2}i} \int d\omega \frac{1}{\omega + i\delta} (-i\omega + \delta)^{-\frac{i\gamma_i\omega}{2\pi}} \\ &\times (i\omega + \delta)^{\frac{i(\gamma_i - 1/2)\omega}{\pi}} \Gamma\left(\frac{1}{2} + \frac{i\omega}{2\pi}\right) \left(\frac{1}{2\pi e}\right)^{-\frac{i\omega}{2\pi}} e^{-i\omega(Q - I_i^{-1})}.\end{aligned}$$

(A13)

We will evaluate each term  $K_{i1/2}$  in turn.

For  $K_{i1}$ , if  $Q < 0$ , we can continue the contour into the upper half plane with the result

$$\begin{aligned}K_{i1}(Q < 0) &= \frac{1}{\pi} \sum_{n=0}^\infty \frac{(-1)^n}{(n + 1/2)\Gamma(n + 1)} \left(\frac{n + 1/2}{e}\right)^{n+1/2} \\ &\times \int_{-\infty}^\infty dq \Delta_{0i}(q) e^{-\pi(2n+1)(g(q) - Q)}.\end{aligned}\quad (\text{A14})$$

If instead  $Q > 0$ , we directly evaluate the integral  $\int dq$ ,

$$\int_{-\infty}^\infty dq \Delta_{0i}(q) e^{i\omega g(q)} \approx e^{i\omega I_i^{-1} - \frac{\tilde{\Gamma}_i \alpha_i}{U_i \Gamma_i} |\omega|}. \quad (\text{A15})$$

Setting  $J_i = I_i^{-1} - Q$  we can then write  $K_{i1}$  as

$$K_{i1} = \frac{i}{\sqrt{2\pi}} \int_{-\infty}^\infty d\omega \frac{e^{i\omega J_i - |\frac{\omega}{2}|(1 + \beta_i^{-1})}}{G^-(\omega)(\omega + i\epsilon)}. \quad (\text{A16})$$

If  $J_i < 0$ , we evaluate this integral by continuing into the lower half plane:

$$\begin{aligned}K_{i1}(Q > 0, J_i < 0) &= 1 - \frac{1}{\pi^{3/2}} \int_0^\infty d\omega \Gamma\left(\frac{1}{2} + \omega\right) \\ &\times \frac{\sin(\pi\omega(1 + \beta_i^{-1}))}{\omega} \left(\frac{e}{\omega}\right)^\omega e^{2\pi J_i \omega} \\ &= 1 - \frac{1 + \beta_i^{-1}}{2\pi J_i} + \mathcal{O}\left(\frac{1}{J_i^2}\right),\end{aligned}\quad (\text{A17})$$

where in the last line we have written down an expansion in  $J_i$  to leading order in  $1/J_i$ . If instead  $J_i > 0$ , i.e.  $0 < Q < I_i^{-1}$ , we close the contour in the upper-half plane obtaining,

$$\begin{aligned}K_{i1} &= \frac{1}{\sqrt{\pi}} \mathbf{P} \int_0^\infty \frac{d\omega}{\omega} \frac{\sin(\pi\beta_i^{-1}\omega)}{\cos(\pi\omega)} \left(\frac{\omega}{e}\right)^\omega \frac{e^{-2\pi J_i \omega}}{\Gamma(\frac{1}{2} + \omega)} \\ &+ \frac{1}{\sqrt{\pi}} \sum_{n=0}^\infty \frac{(-1)^n}{n + \frac{1}{2}} \left(\frac{n + \frac{1}{2}}{e}\right)^{n+\frac{1}{2}} \\ &\times \frac{\cos(\pi\beta_i^{-1}(n + \frac{1}{2})) e^{-2\pi J_i(n + \frac{1}{2})}}{\Gamma(1 + n)},\end{aligned}\quad (\text{A18})$$

where the symbol  $\mathbf{P}$  indicates that the principal value of the integral is to be taken. We can alternatively evaluate this integral and sum in a fashion similar to that used in Refs. (35) and (36) to obtain,

$$\begin{aligned}K_{i1}(Q > 0, J_i > 0) &= \sqrt{2} - 1 - \frac{\pi}{\sqrt{26}} J_i + \frac{\pi^2 \sqrt{2}}{24^2} J_i^2 \\ &+ \frac{1}{\sqrt{2}\pi} (\beta_i^{-1} - 1) J_i + \mathcal{O}((\beta_i^{-1} - 1)^2 J_i) + \mathcal{O}(J_i^3).\end{aligned}\quad (\text{A19})$$

We similarly evaluate  $K_{i2}$  for  $J_i > 0$  and  $J_i < 0$ . For  $J_i > 0$  we can continue into the upper half plane with the result

$$K_{i2}(J_i > 0) = \frac{\text{sign}(1 - \beta_i)}{\sqrt{\pi}} \mathbf{P} \int_0^\infty d\omega \left(\frac{\omega}{e}\right)^\omega e^{2\pi J_i \omega}$$

$$\begin{aligned}
& \times \frac{1}{\Gamma(\frac{1}{2} + \omega) \cos(\pi\omega)} \frac{\sin(2\pi\omega(\gamma_i - \frac{1}{2}))}{\omega} \\
& + \frac{\text{sign}(1 - \beta_i)}{\sqrt{\pi}} \sum_{n=0}^{\infty} \frac{(-1)^n}{n + \frac{1}{2}} \left( \frac{n + \frac{1}{2}}{e} \right)^{n + \frac{1}{2}} \\
& \times \frac{e^{-2\pi J_i \omega} \cos(\pi(2n + 1)(\gamma_i - \frac{1}{2}))}{\Gamma(1 + n)} \\
& = \frac{\text{sign}(1 - \beta_i)(\gamma_i - 1/2)}{\pi J_i} + \mathcal{O}\left(\frac{1}{J_i^2}\right). \quad (\text{A20})
\end{aligned}$$

And if  $J_i < 0$ , we instead continue into the lower half plane with the result,

$$\begin{aligned}
K_{i2}(J_i < 0) &= \text{sign}(1 - \beta_i) \left( 1 - \frac{1}{\pi^{3/2}} \int_0^{\infty} d\omega e^{2\pi J_i \omega} \right. \\
& \times \left. \left( \frac{\omega}{\omega} \right)^{\omega} \Gamma\left(\frac{1}{2} + \omega\right) \frac{\sin(2\pi\omega\gamma_i)}{\omega} \right) \\
& = \text{sign}(1 - \beta_i) \left( 1 - \frac{\gamma_i}{\pi |J_i|} \right) + \mathcal{O}\left(\frac{1}{J_i^2}\right). \quad (\text{A21})
\end{aligned}$$

We now finally turn to how  $Q$  depends on  $U_i$ ,  $\Gamma_i$  and  $\epsilon_{di}$ . As the bulk density equations are the same as for a single dot, this dependence can be taken directly from Refs. (35) and (36). If  $Q < 0$ ,  $Q$  is determined implicitly by the equation

$$\frac{2\epsilon_{di} + U_i}{\sqrt{2U_i\Gamma_i}} = \frac{\sqrt{2}}{\pi} \sum_{n=0}^{\infty} \frac{(-1)^n e^{\pi Q(2n+1)}}{(2n+1)^{3/2}} G^+(i\pi(2n+1)). \quad (\text{A22})$$

If further  $Q \gg 0$ ,  $Q$  is given by

$$\begin{aligned}
Q &= q^* + \frac{1}{2\pi} \ln(2\pi e q^*) \\
\sqrt{q^*} &= \frac{\epsilon_{di} + U_i/2}{\sqrt{2U_i\Gamma_i}}. \quad (\text{A23})
\end{aligned}$$

We note that there are no inconsistencies in the above equations as the quantities  $2U_i\Gamma_i$  and  $U_i + 2\epsilon_{di}$  are independent of  $i = 1, 2$ .

### 3. Analysis of Finite Field Equations

The equation we must solve takes the form

$$\rho_i^{\text{imp}}(q) = \rho_{0i}^{\text{imp}}(q)$$

$$-g'(q) \int_{-\infty}^B d\lambda' R(g(q') - g(q)) \rho_i^{\text{imp}}(q'). \quad (\text{A24})$$

As we are interested in the behaviour of  $\rho_i^{\text{imp}}(q)$  at  $q < 0$ , we introduce the change of variables  $z = g(q)$  for  $z > 0$  and  $q < 0$  and define  $\rho_i^{\text{imp}}(z) = -\rho_i^{\text{imp}}(q)/g'(q)$ . The above equation is then recast as

$$\rho_i^{\text{imp}}(z) = \rho_{0i}^{\text{imp}}(z) + \int_b^{\infty} dz R(z - z') \rho_i^{\text{imp}}(z'), \quad (\text{A25})$$

where  $b = B^2/(2U_i\Gamma_i)$  and we can write the Fourier transform of  $\rho_{0i}^{\text{imp}}(z)$  as

$$\begin{aligned}
\rho_{0i}^{\text{imp}}(\omega) &= \int d\omega e^{i\omega z} \rho_{0i}^{\text{imp}}(z) \\
&= \Theta(\beta_i - 1) \frac{\cosh(\omega(\frac{1}{2} - \frac{1}{2\beta_i})) e^{i\omega I_i^{-1}}}{\cosh(\frac{\omega}{2})} \\
&+ \frac{i}{2} \tanh \frac{\omega}{2} \int dq e^{i\omega g(q)} \Delta_{0i}(q). \quad (\text{A26})
\end{aligned}$$

The kernel,  $R(z)$ , of the integral equation in Eqn. (A25) is the same encountered in analyzing the scattering phase at zero field. Thus using the analysis at the beginning of this Appendix together with the properties of  $R(z)$  already established, we can immediately write down the form of  $\rho_i^{\text{imp}}(z)$ :

$$\int_{-\infty}^B dq \rho_i^{\text{imp}}(q) = \frac{G_+(0)}{2\pi i} \int_{-\infty}^{\infty} d\omega \frac{e^{-i\omega b} \rho_{0i}^{\text{imp}}(\omega) G_-(\omega)}{\omega - i\delta}. \quad (\text{A27})$$

Substituting in the above form for  $\rho_{0i}^{\text{imp}}(\omega)$ , we obtain the solution as written in Eqn. (4.28). As discussed in Section V.B, the Fermi surface parameter,  $b$ , is the same as found in the analysis of the Anderson model for single level dots and for small fields takes the form  $b = -\frac{1}{2\pi} \log \frac{\pi e H^2}{4U_i\Gamma_i}$ .

<sup>1</sup> D. Goldhaber-Gordon et al. PRL **81**, 5225 (1998); D. Goldhaber-Gordon et al., Nature **391**, 156 (1998).

<sup>2</sup> S. Cronenwett et al., Science **281**, **540**, (1998); W.G. van der Wiel et al., Science **289**, 2105 (2000).

<sup>3</sup> M. Eto and Y. Nazarov, Phys. Rev. Lett. **85**, 1306 (2000).

<sup>4</sup> M. Pustilnik, L. I. Glazman, Phys. Rev. Lett. **87**, 216601

(2001).

<sup>5</sup> M. Pustilnik, L. I. Glazman, Phys. Rev. Lett. **85**, 2993 (2000).

<sup>6</sup> W.G. van der Wiel, S. De Franceschi, J.M. Elzerman, S. Tarucha, L.P. Kouwenhoven, J. Motohisa, F. Nakajima, T. Fukui, Phys. Rev. Lett. **88**, 126803 (2002).

- <sup>7</sup> H. Jeong, A. M. Chang, and M. R. Melloch, *Science* **293**, 2221 (2001).
- <sup>8</sup> N. J. Craig, J. M. Taylor, E. A. Lester, C. M. Marcus, M. P. Hanson, and A. C. Gossard, *Science* **304**, 565 (2004).
- <sup>9</sup> J. R. Petta, A. C. Johnson, J. M. Taylor, E. A. Laird, A. Yacoby, M. D. Lukin, C. M. Marcus, M. P. Hanson, and A. C. Gossard, *Science* **309**, 2180 (2005).
- <sup>10</sup> F. H. L. Koppens, J. A. Folk, J. M. Elzerman, R. Hanson, L. H. Willems van Beveren, I. T. Vink, H. P. Tranitz, W. Wegscheider, L. P. Kouwenhoven, and L. M. K. Vandersypen, *Science* **309**, 1346 (2005).
- <sup>11</sup> N. Mason, M. J. Biercuk, and C. M. Marcus, *Science* **303**, 655 (2004).
- <sup>12</sup> Sami Sapmaz, Carola Meyer, Piotr Beliczynski, Pablo Jarillo-Herrero, and Leo P. Kouwenhoven, *Nano Lett.* **6** 1350 (2006).
- <sup>13</sup> A. C. Johnson, J. R. Petta, J. M. Taylor, A. Yacoby, M. D. Lukin, C. M. Marcus, M. P. Hanson, A. C. Gossard, *Nature* **435** 925 (2005).
- <sup>14</sup> J. Taylor, J. Petta, A. Johnson, A. Yacoby, C. Marcus, and M. Lukin, *cond-mat/0602470*.
- <sup>15</sup> A. S. Bracker, E. A. Stinaff, D. Gammon, M. E. Ware, J. G. Tischler, A. Shabae, Al. L. Efros, D. Park, D. Gershoni, V. L. Korenev, and I. A. Merkulov, *Phys. Rev. Lett.* **94**, 047402 (2005).
- <sup>16</sup> R. Lopez, D. Sanchez, M. Lee, M.-S. Choi, P. Simon, and K. Le Hur, *Phys. Rev. B* **71**, 115312 (2005).
- <sup>17</sup> R. Lopez, R. Aguado, and G. Platero, *Phys. Rev. Lett.* **89**, 136802 (2002).
- <sup>18</sup> Y. Tanaka and N. Kawakami, *Phys. Rev. B* **72**, 085304 (2005).
- <sup>19</sup> E. Vernek, N. Sandler, S. E. Ulloa, E. V. Anda, *cond-mat/0511226*.
- <sup>20</sup> C.A. Büsser, G.B. Martins, K.A. Al-Hassanieh, Adriana Moreo, and Elbio Dagotto, *Phys. Rev. B* **70**, 245303 (2004).
- <sup>21</sup> D. Boese, W. Hofstetter, and H. Schoeller, *Phys. Rev. B* **66**, 125315 (2002).
- <sup>22</sup> V. Kashcheyevs, A. Schiller, A. Aharony, O. Entin-Wohlman, *cond-mat/0610194*.
- <sup>23</sup> M. Vavilov, L. Glazman, *Phys. Rev. Lett.* **94**, 086805 (2005).
- <sup>24</sup> P. S. Cornaglia and D. R. Grempel, *Phys. Rev. B* **71**, 075305 (2005).
- <sup>25</sup> P. Simon, R. Lopez, and Y. Oreg, *Phys. Rev. Lett.* **94**, 086602 (2005).
- <sup>26</sup> A. Georges and Y. Meir, *Phys. Rev. Lett.* **82**, 3508 (1999).
- <sup>27</sup> A. Posazhennikova and P. Coleman, *Phys. Rev. Lett.* **94**, 036802 (2005).
- <sup>28</sup> L. Dias da Silva, N. P. Sandler, K. Ingersent, and S. Ulloa, *Phys. Rev. Lett.* **97**, 096603 (2006).
- <sup>29</sup> M. Choi, R. Lopez, and R. Aguado, *Phys. Rev. Lett.* **95**, 067204 (2005).
- <sup>30</sup> G. B. Martins, C. A. Büsser, K. A. Al-Hassanieh, A. Moreo, E. Dagotto, *Phys. Rev. Lett.* **94**, 026804 (2005).
- <sup>31</sup> P. G. Silvestrov and Y. Imry, *cond-mat/0609355*.
- <sup>32</sup> K. Kikoin and Y. Oreg, *cond-mat/0610207*.
- <sup>33</sup> V. Meden and F. Marquardt, *Phys. Rev. Lett.* **96**, 146801 (2006).
- <sup>34</sup> C. Karrasch, T. Hecht, A. Weichselbaum, J. von Delft, Y. Oreg, V. Meden, *cond-mat/0612490*.
- <sup>35</sup> P. Wiegmann, V. Filyov, and A. Tsvelik, *Sov. Phys. JETP Lett.* **35** (1982) 77; A. Tsvelik and P. Wiegmann, *Adv. in Phys.* **32** (1983) 453. N. Kawakami and A. Okiji, *Phys. Lett. A* **86**, 483 (1981).
- <sup>36</sup> R. M. Konik, H. Saleur, and A.W.W. Ludwig, *PRL* **87**, 236801 (2001); *ibid*, *PRB* **66**, 125304 (2002).
- <sup>37</sup> R. M. Konik, *cond-mat/0602617*.
- <sup>38</sup> P. Simon and D. Feinberg, *Phys. Rev. Lett.* **97**, 247207 (2006).
- <sup>39</sup> C. Kittel, *Solid State Physics* (Academic Press, New York, 1968), Vol. 22.
- <sup>40</sup> Y. Utsumi, J. Martinek, P. Bruno, and H. Imamura, *Phys. Rev. B* **69**, 155320 (2004).
- <sup>41</sup> R. M. Konik, *J. Stat. Mech.* (2004) L11001; *ibid*, *cond-mat/0401617*.
- <sup>42</sup> N. Andrei, *Phys. Lett. A* **87**, 299 (1982).
- <sup>43</sup> D. Haldane, T. Choy, *Phys. Lett. A* **90**, 83 (1981).
- <sup>44</sup> T. Deguchi, F. Essler, F. Göhmann, A. Klümper, V. Korepin, K. Kusakabe, *Physics Reports* **331**, (2000) 197.
- <sup>45</sup> S.Y. Cho, H.Q. Zhou and R.H. McKenzie, *Phys. Rev. B* **68**, 125327 (2003).
- <sup>46</sup> P. Simon and I Affleck, *Phys. Rev. B* **68**, 115304 (2003).
- <sup>47</sup> N. Kawakami and A. Okiji, *Phys. Rev. B* **40** 7066 (1989).
- <sup>48</sup> B. A. Jones, B. G. Kotliar, and A. J. Millis, *Phys. Rev. B* **39**, 3415 (1989).
- <sup>49</sup> D. Haldane, *Phys. Rev. Lett.* **40**, 416 (1978).
- <sup>50</sup> T. Costi, A. Hewson, and V. Vlatić, *J. Phys.: Cond. Mat.* **6**, 2519 (1994).
- <sup>51</sup> D. Langreth, *Phys. Rev.* **150**, 516 (1966).
- <sup>52</sup> M. Goldstein and R. Berkovits, *cond-mat/0610810*.
- <sup>53</sup> J. König, Y. Gefen, and G. Schön, *Phys. Rev. Lett.* **81**, 4468 (1998).
- <sup>54</sup> A. Kaminski, Y. Nazarov, and L. Glazman, *Phys. Rev. B* **62**, 8154 (2000).
- <sup>55</sup> K. Majumdar, A. Schiller, and S. Hershfield, *Phys. Rev. B* **57**, 2991 (1998).
- <sup>56</sup> M. Pustilnik and L. Glazman, *Phys. Rev. Lett.* **87**, 216601 (2001).